(12) INTERNATIONAL APPLICATION PUBLISHED UNDER THE PATENT COOPERATION TREATY (PCT)

(19) World Intellectual Property Organization
International Bureau

(43) International Publication Date
14 November 2013 (14.11.2013)

WIPO | PCT

(10) International Publication Number
WO 2013/170249 A1

(51) International Patent Classification:
B01D 69/12 (2006.01) *B01D 69/10* (2006.01)
B01D 71/02 (2006.01)

(21) International Application Number:
PCT/US2013/040744

(22) International Filing Date:
13 May 2013 (13.05.2013)

(25) Filing Language: English

(26) Publication Language: English

(30) Priority Data:
61/645,944 11 May 2012 (11.05.2012) US

(71) Applicants: **VIRGINIA TECH INTELLECTUAL PROPERTIES, INC.** [US/US]; 2200 Kraft Drive, Suite 1050, Blacksburg, VA 24060 (US). **UNIVERSITY OF PITTSBURGH - OF THE COMMONWEALTH SYSTEM OF HIGHER EDUCATION** [US/US]; 200 Gardner Steel Conference Center, Pittsburgh, PA 15260 (US).

(72) Inventors: **MARAND, Eva**; 3670 Deer Run Road, Blacksburg, VA 24060 (US). **SURAPATHI, Anil, K.**; 7108 NE Ronler Way, Apt. 2822, Hillsboro, OR 97124 (US). **CHEN, Wai, Fong**; 911 University City Blvd., Apt. A13, Blacksburg, VA 24060 (US). **JOHNSON, Karl**; 1249 Benedum Hall, Pittsburgh, PA 15261 (US). **CHEN, Hangyan**; 2715 Murray Ave, Apt. 725, Pittsburgh, PA 15217 (US).

(74) Agent: **MAYBERRY, Michele, L.**; New River Valley IP Law, P.O. Box 10944, Blacksburg, VA 24062 (US).

(81) Designated States *(unless otherwise indicated, for every kind of national protection available)*: AE, AG, AL, AM, AO, AT, AU, AZ, BA, BB, BG, BH, BN, BR, BW, BY, BZ, CA, CH, CL, CN, CO, CR, CU, CZ, DE, DK, DM, DO, DZ, EC, EE, EG, ES, FI, GB, GD, GE, GH, GM, GT, HN, HR, HU, ID, IL, IN, IS, JP, KE, KG, KM, KN, KP, KR, KZ, LA, LC, LK, LR, LS, LT, LU, LY, MA, MD, ME, MG, MK, MN, MW, MX, MY, MZ, NA, NG, NI, NO, NZ, OM, PA, PE, PG, PH, PL, PT, QA, RO, RS, RU, RW, SC, SD, SE, SG, SK, SL, SM, ST, SV, SY, TH, TJ, TM, TN, TR, TT, TZ, UA, UG, US, UZ, VC, VN, ZA, ZM, ZW.

(84) Designated States *(unless otherwise indicated, for every kind of regional protection available)*: ARIPO (BW, GH, GM, KE, LR, LS, MW, MZ, NA, RW, SD, SL, SZ, TZ, UG, ZM, ZW), Eurasian (AM, AZ, BY, KG, KZ, RU, TJ, TM), European (AL, AT, BE, BG, CH, CY, CZ, DE, DK, EE, ES, FI, FR, GB, GR, HR, HU, IE, IS, IT, LT, LU, LV, MC, MK, MT, NL, NO, PL, PT, RO, RS, SE, SI, SK, SM, TR), OAPI (BF, BJ, CF, CG, CI, CM, GA, GN, GQ, GW, ML, MR, NE, SN, TD, TG).

[Continued on next page]

(54) Title: FUNCTIONALIZED CARBON NANOTUBE NANOCOMPOSITE MEMBRANES AND METHODS OF THEIR FABRICATION

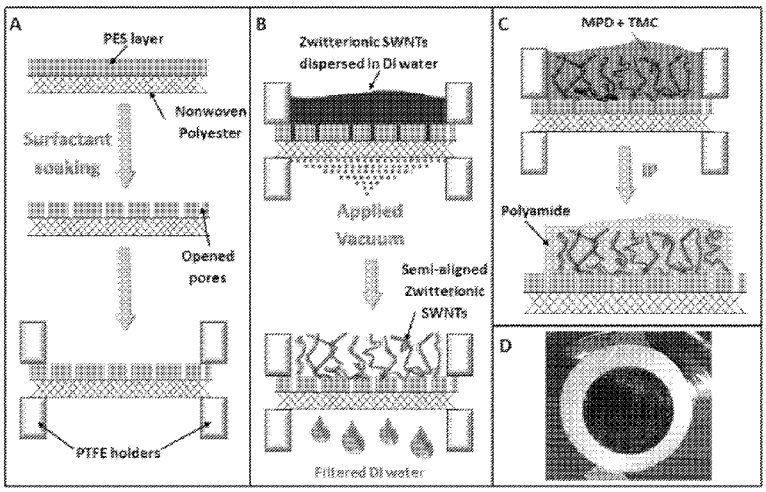

FIGS. 3A-D

(57) Abstract: Functionalized carbon nanotube nanocomposite membrane and methods of making them are provided. The nanocomposite membranes are made from functionalized carbon nanotubes deposited on a membrane support that is overlayed with a polymer matrix such as polyamide. The carbon nanotubes may be functionalized with a variety of functional groups, such as short zwitterionic functional groups. Methods for functionalization of carbon nanotubes, deposition of carbon nanotubes on a membrane support, and interfacial polymerization of polyamide are also described. The methods of the invention may be carried out on an industrial level and provide for membranes with high water transport and salt rejection and resistance to biofouling, which may be particularly useful for desalination applications.

WO 2013/170249 A1

Declarations under Rule 4.17:

— *of inventorship (Rule 4.17(iv))*

Published:

— *with international search report (Art. 21(3))*

FUNCTIONALIZED CARBON NANOTUBE NANOCOMPOSITE MEMBRANES AND METHODS OF THEIR FABRICATION

Cross-Reference to Related Applications

[0001] This application claims priority to and the benefit of the filing date of U.S. Provisional Application No. 61/645,944, filed on May 11, 2012, which is hereby incorporated by reference herein in its entirety.

STATEMENT OF GOVERNMENT INTEREST

[0002] This invention was made with government support under Agreement Number R10AP81214 awarded by United States Department of the Interior, Bureau of Reclamation. The government has certain rights in the invention.

BACKGROUND OF THE INVENTION

Field of the Invention

[0003] The present invention relates to membranes for use in desalination and other applications, as well as to methods of fabricating such membranes. More particularly, embodiments of the invention relate to zwitterion-functionalized carbon nanotube nanocomposite membranes and methods of their fabrication.

Description of the Related Art

[0004] Approximately 800 million people living on the earth do not have access to safe drinking water. *See* WHO/UNICEF, Progress on Drinking Water and Sanitation 2012, 1-58, http://www.who.int/water_sanitation_ health/ publications/2012/jmp_report/e n/ (2012). Moreover, almost one quarter of people on the earth live in areas where the ground water is being depleted faster than it can be replaced. *See* Gleeson, T.; Wada, Y.; Bierkens, M. F. P.; van Beek, L. P. H., Water balance of global aquifers revealed by groundwater footprint, Nature, 488, 197-200 (2012). Although over 70% of the surface of the earth is covered with water, access to clean water remains a critical issue worldwide. *See* Gleick, P. H., Water Resources, in Encyclopedia of Climate and

Weather Schneider, S. H., Ed. Oxford University Press: New York, Vol. 2, pp. 817-823 (1996). Clearly, finding a way to desalinate seawater, clean up brackish water, and remove harmful ions from contaminated water at low cost in a sustainable way would be a major step toward solving much of the world's water problems.

[0005] Conventional methods for desalination include distillation and reverse osmosis. The first method is unavoidably energy intensive, as water has a very high heat of vaporization. Reverse osmosis with semi-permeable polymer membranes is an attractive option, but there is a need to improve the permeance of water, while keeping the salt rejection ratio at acceptable levels. Additionally, biofouling of RO membranes is a major problem, causing both reduced flux and high maintenance costs. *See* Al-Ahmad, M.; Aleem, F. A. A.; Mutiri, A.; Ubaisy, A., Biofuoling in RO membrane systems Part 1: Fundamentals and control, Desalination, 132, 173-179. (2000).

[0006] Carbon nanotubes are promising materials for use in membranes because they have been shown to exhibit remarkably high flux. (*See* Holt, J. K.; Park, H. G.; Wang, Y.; Stadermann, M.; Artyukhin, A. B.; Grigoropoulos, C. P.; Noy, A.; Bakajin, O., Fast Mass Transport Through Sub-2-Nanometer Carbon Nanotubes, Science, 312, 1034-1037 (2006) ("Holt *et al.*, 2006"); and *see* Kim, S.; Chen, L.; Johnson, J. K.; Marand, E., Polysulfone and Functionalized Carbon Nanotube Mixed Matrix Membranes for Gas Separation: Theory and Experiment. J. Membr. Sci., 294, 147-158 (2007); and *see* Kim, S.; Jinschek, J. R.; Chen, H.; Sholl, D. S.; Marand, E., Scalable fabrication of carbon nanotube/polymer nanocomposite membranes for high flux transport, Nano Lett., 7, 2806-2811 (2007) ("Kim, Jinschek, Chen, Sholl, and Marland, 2007"); and *see* Majumder, M.; Chopra, N.; Andrews, R.; Hinds, B. J., Nanoscale hydrodynamics - Enhanced flow in carbon nanotubes, Nature, 438, 44-44 (2005) ("Majumder, Chopra, Andrews, and Hinds, 2005"); and *see* Majumder, M.; Chopra, N.; Hinds, B. J., Effect of tip functionalization on transport through vertically oriented carbon nanotube membranes, J. Am. Chem. Soc. 127, 9062-9070 (2005) ("Majumder,

Chopra, and Hinds, 2005"); and *see* Skoulidas, A. I.; Ackerman, D. M.; Johnson, J. K.; Sholl, D. S., Rapid Transport of Gases in Carbon Nanotubes, Phys. Rev. Lett., 89, 185901. (2002); and *see* Skoulidas, A. I.; Sholl, D. S.; Johnson, J. K., Adsorption and diffusion of carbon dioxide and nitrogen through single-walled carbon nanotube membranes, J. Chem. Phys., 124, 054708. (2006) ("Skoulidas *et al.*, 2006"); and *see* Surapathi, A.; Herrera-Alonso, J.; Rabie, F.; Martin, S.; Marand, E., Fabrication and gas transport properties of SWNT/polyacrylic nanocomposite membranes, J. Membr. Sci., 375, 150-156 (2011); and *see* Majumder, M.; Chopra, N.; Hinds, B. J., Mass Transport through Carbon Nanotube Membranes in Three Different Regimes: Ionic Diffusion and Gas and Liquid Flow, ACS Nano, 5, 3867-3877 (2011) ("Majumbder *et al.*, 2011").

[0007] Molecular simulations and experimental studies have shown that the transport of fluids through carbon nanotubes is orders of magnitude faster than through other nanoporous materials due to the unprecedented smoothness and regularity of the carbon nanotube pores. *See* Holt *et al.*, 2006; and *see* Majumder, Chopra, Andrews, and Hinds, 2005; and *see* Majumder, Chopra, and Hinds, 2005; and *see* Skoulidas *et al.*, 2006; and *see* Holt, J. K., Carbon Nanotubes and Nanofluidic Transport, Advanced Materials, 21, 3542-3550 (2009); and *see* Holt, J. K.; Koy, A.; Huser, T.; Eaglesham, D.; Bakajin, O., Fabrication of a carbon nanotube-embedded silicon nitride membrane for studies of nanometer-scale mass transport, Nano Lett., 4, 2245-2250 (2004); and *see* Skoulidas, A. I.; Sholl, D. S., Transport Diffusivities of CH_4, CF_4, He, Ne, Ar, Xe, and SF_6 in Silicalite from Atomistic Simulations, J. Phys. Chem., 106, 5058-5067 (2002); and *see* Kalra, A.; Garde, S.; Hummer, G., Osmotic water transport through carbon nanotube membranes, PNAS, 100, 10175-10180 (2003).

[0008] It has been suggested that the transport of water through sub-nanometer carbon nanotubes occurs by way of a cooperative, pulse-like movement of hydrogen-bonded molecules within the channel, similar to what has been observed in aquaporin biological channels. *See* Zhu, F.; Tajkhorshid, E.; Schulten, K., Theory and Simulation of Water Permeation in Aquaporin-1,

Biophys. J., 86, 50-57 (2004). The transport of water in carbon nanotubes has been shown to give flow rates that are faster than predicted by classical hydrodynamics. *See* Thomas, J. A.; McGaughey, A. J. H., Water Flow in Carbon Nanotubes: Transition to Subcontinuum Transport, Phys. Rev. Lett., 102, 184502-184502 (2009). Thomas, J. A.; McGaughey, A. J. H., Reassessing Fast Water Transport Through Carbon Nanotubes, Nano Lett., 8, 2788-2793 (2008). The enhanced water transport together with carbon nanotube pore diameters on the order of nanometers opens the possibility of employing carbon nanotubes to filter ions from water. Molecular dynamics (MD) simulation studies (*See* Corry, B., Designing carbon nanotube membranes for efficient water desalination, Journal of Physical Chemistry B, 112, 1427-1434 (2008); and *see* Song, C.; Corry, B., Intrinsic Ion Selectivity of Narrow Hydrophobic Pores, J. Phys. Chem. B, 113, 7642-7649 (2009)) have examined the ability of carbon nanotubes with diameters ranging from 0.6 to 1.1 nm to filter ions from water. These results indicated that ions can be almost completely excluded from pores up to 0.9 nm in diameter due to ion desolvation energy barriers. By contrast, water faces relatively low energy barriers and is able to pass through these small nanotubes, but at flow rates that are much lower than in larger nanotubes because water transport in these narrow carbon nanotubes is limited to single-file flow. Larger diameter carbon nanotubes have much higher water flux, but do not have the ability to reject ions. For example, Yu *et al.* also studied ion transport through carbon nanotube membranes using larger diameter (3 nm) carbon nanotubes. *See* Yu, M.; Funke, H. H.; Falconer, J. L.; Noble, R. D., Gated Ion Transport through Dense Carbon Nanotube Membranes, J. Am. Chem. Soc., 132, 8285-8290 (2010) ("Yu *et al.*, 2010"). These larger diameter nanotubes did not exhibit any ion rejection properties, but did display gated transport due to water wettability, that could be tuned by temperature, sonication, or addition of solutes (Yu *et al.*, 2010).

[0009] Carbon nanotubes with pore diameters down to 0.4 nm have been reported (*See* Sun, L. F.; Xie, S. S.; Liu, W.; Zhou, W. Y.; Liu, Z. Q.; Tang, D. S.;

Wang, G.; Qian, L. X., Materials: Creating the narrowest carbon nanotubes, Nature, 403, 384-384 (2000)) so that it is at least in principle possible to produce nanotubes that would reject ions by size exclusion. *See* Cannon, J.; Kim, D.; Maruyama, S.; Shiomi, J., Influence of Ion Size and Charge on Osmosis, J. Phys. Chem. B, 116, 4206-4211 (2012). However, experimentally produced carbon nanotubes have a range of diameters and it is currently not possible to economically separate out nanotubes having a very narrow diameter distribution, so that producing membranes with carbon nanotubes having diameters < 0.9 nm is not currently practical. An alternate approach to requiring very small diameter carbon nanotubes is to tune the effective diameter of the carbon nanotube entrance by attaching functional groups. Experimental work on ionic flux through functionalized carbon nanotubes has been reported by Hinds *et al.* (*See* Hinds, B. J.; Chopra, N.; Rantell, T.; Andrews, R.; Gavalas, V.; Bachas, L. G., Aligned multiwalled carbon nanotube membranes, Science, 303, 62-65 (2004). ("Hinds et. al, 2004)") who showed that biotin functionalized carbon nanotubes showed a marked reduction of $Ru(NH_3)6+$ and by Majumder and coworkers who studied voltage gated carbon nanotube membranes formed by tethering charged molecules to the ends of large-diameter carbon nanotubes. *See* Majumder, M.; Zhan, X.; Andrews, R.; Hinds, B. J., Voltage Gated Carbon Nanotube Membranes, Langmuir, 23, 8624-8631 (2007) ("Majumder *et al.*, 2007"). Their work has focused on studying transport of two different sized but equally charged molecules, ruthenium bipyridine and methyl viologen, through multi-walled carbon nanotubes with 7-nm nominal core diameters. They showed that flux and selectivity could be changed by applying a voltage across the membrane and that this result is consistent with the charged functional groups being drawn into the carbon nanotubes at positive bias, causing a modulation of the pore size (Majumbder *et al.*, 2007). Similarly, tip and core functionalization of large diameter carbon nanotubes has been shown to modulate the flux of water, both experimentally (Majumbder, 2011) and from simulations. *See* Majumder, M.; Corry, B., Anomalous decline of water transport in covalently modified carbon nanotube membranes, Chemical Communications, 47, 7683-7685 (2011).

Fornasiero *et al.* studied ion exclusion in carbon nanotubes functionalized with hydroxyl, carbonyl and carboxylic groups having pores less than 2 nm in diameter as a function of solution ionic strength, pH, and ion valence. *See* Fornasiero, F.; Bin In, J.; Kim, S.; Park, H. G.; Wang, Y.; Grigoropoulos, C. P.; Noy, A.; Bakajin, O., pH-Tunable Ion Selectivity in Carbon Nanotube Pores, Langmuir, 26, 14848-14853 (2010); *see* also Fornasiero, F.; Park, H. G.; Holt, J. K.; Stadermann, M.; Grigoropoulos, C. P.; Noy, A.; Bakajin, O., Ion exclusion by sub-2-nm carbon nanotube pores, Proc. Natl. Acad. Sci. U.S.A., 105, 17250-17255 (2008) ("Fornasiero *et al.*, 2008"). Their results suggest a Donnan-type rejection mechanism, dominated by electrostatic interactions between the fixed COO- charges on the ends of the carbon nanotubes and mobile ions. However, this also means that the rejection ratios decreased significantly at higher electrolyte concentrations. The hydrated radii of the ions (~0.6 nm) were significantly smaller than the carbon nanotube pore radius (~1.6 nm) and therefore separation of ions by size exclusion was not possible. Atomistic simulations by Corry predicted that ion rejection can take place in carbon nanotubes having 1.1 nm diameters through the addition of functional groups having charged moieties. *See* Corry, B., Water and ion transport through functionalised carbon nanotubes: implications for desalination technology, Energy Environ, Sci., 4, 751-759 (2011) ("Corry, 2011"). The charged groups prevent like-charged ions from entering the tube due to electrostatic repulsion. Oppositely charged ions are attracted to the functional groups. Corry found that a high concentration of charged groups, such as 8 COO- groups on a carbon nanotube of diameter 1.1 nm, completely blocks the transport of both positive and negative ions (Corry, 2011). Chen *et al.* used simulations to design an asymmetric tip functionalized carbon nanotube membrane for salt rejection. *See* Chen, Q. W.; Meng, L. Y.; Li, Q. K.; Wang, D.; Guo, W.; Shuai, Z. G.; Jiang, L., Water Transport and Purification in Nanochannels Controlled by Asymmetric Wettability, Small, 7, 2225-2231 (2011). The driving force supplied by hydrophilic–hydrophobic ends in smaller tubes (6,6) and (8,8) induced the transport of water while ions were always blocked. Use of larger diameter

nanotubes increased the water permeance over narrow carbon nanotubes, although the addition of a large number of functional groups reduced the water flux by about a factor of 5. Simulations by Won *et al.* of nanotubes having charges on the walls of the carbon nanotubes indicate that the free energy of both water and ions inside the carbon nanotubes are affected by the charges. *See* Won, C. Y.; Joseph, S.; Aluru, N. R., Effect of quantum partial charges on the structure and dynamics of water in single-walled carbon nanotubes, J. Chem. Phys., 125, 114701-114701 (2006). This is consistent with the idea that charges affect the free energy barrier for water and ions entering nanotubes. Joseph *et al.* used MD simulations to explore the occupancy of ions in narrow carbon nanotube channels when partial charges were placed on the rim atoms of the nanotubes and an external field was applied along the nanotube axis. *See* Joseph, S.; Aluru, N. R., Why are carbon nanotubes fast transporters of water? Nano Lett., 8, 452-458 (2008). The simulation results showed that the ion occupancy in a carbon nanotube solvated in an electrolyte was very low for neutral nanotubes and increased significantly in the presence of charged functionalities. Suk and Aluru have shown that the application of electric fields to nanotubes affects the flux of water under applied pressure for (6,6) carbon nanotubes. *See* Suk, M. E.; Aluru, N. R., Effect of induced electric field on single-file reverse osmosis. Phys. Chem. Chem. Phys., 11, 8614-8619 (2009). Therefore, charged groups at the ends of carbon nanotubes, which generate electric fields, will also perturb the flux of water. *See* Joseph, S.; Mashl, R. J.; Jakobsson, E.; Aluru, N. R., Electrolytic transport in modified carbon nanotubes, Nano Lett., 3, 1399-1403 (2003). Simulation studies on (10,10) boron nitride nanotubes versus (10,10) carbon nanotubes show reversed selectivity of K^+ and Cl^- ions due to different entrance effects that result from the difference in charges at the entrance of the nanotubes. *See* Won, C. Y.; Aluru, N. R., A chloride ion-selective boron nitride nanotube, Chem. Phys. Lett., 478, 185-190 (2009). Hughes *et al.* studied the effect of tip functionalization on water flow through narrow (6,6) and (8,8) carbon nanotubes. *See* Hughes, Z. E.; Shearer, C. J.; Shapter, J.; Gale, J. D., Simulation of Water Transport Through Functionalized

Single-Walled Carbon Nanotubes (SWCNTs), The Journal of Physical Chemistry C, 116, 24943-24953 (2012) ("Hughes *et al.*, 2012"). They compared water diffusion as a function of tip functionalization using hydrogen, hydroxyl, carboxylic acid, and carboxylate functional groups. They found that polar functional groups act to slow water diffusion (Hughes *et al.*, 2012). These experimental and simulation studies clearly demonstrate the possibility of tuning ion and water transport through functionalizing the entrance of carbon nanotubes.

[00010] It is noted that nanoporous graphene is a system that is similar to carbon nanotubes; both are one-atom thick materials composed of carbon. Atomistic simulations have been used to predict that porous graphene could also be used for desalination by tuning the size of the pores. *See* Sint, K.; Wang, B.; Král, P., Selective Ion Passage through Functionalized Graphene Nanopores, Journal of the American Chemical Society, 130, 16448-16449 (2008). Cohen-Tanugi, D.; Grossman, J. C., Water Desalination across Nanoporous Graphene, Nano Letters, 12, 3602-3608 (2012) ("Cohen-Tanugi and Grossman, 2012").

[00011] Carbon nanotubes functionalized with chain-like zwitterion groups have great promise in being more effective at rejecting both positive and negative ions than carbon nanotubes having singly charged functional groups. It is believed that this enhanced performance is due to a combination of Donnan-type rejection and steric hindrance, because the zwitterion groups are larger and have more conformational degrees of freedom than the functional groups considered in previous simulations (Corry, 2011). Moreover, in embodiments of the invention zwitterionic groups can be used to prevent biofouling, which is a major problem with current desalination membranes, since zwitterion-treated surfaces have been shown to be resistant to both cell adhesion and biofouling. (*See* Cheng, G.; Li, G. Z.; Xue, H.; Chen, S. F.; Bryers, J. D.; Jiang, S. Y., Zwitterionic carboxybetaine polymer surfaces and their resistance to long- term biofilm formation, Biomaterials, 30, 5234-5240 (2009); and *see* Ladd, J.; Zhang, Z.; Chen, S.; Hower, J. C.; Jiang, S., Zwitterionic polymers exhibiting high resistance to nonspecific protein adsorption from human serum and plasma,

Biomacromolecules, 9, 1357-1361, (2008); and *see* Li, G. Z.; Cheng, G.; Xue, H.; Chen, S. F.; Zhang, F. B.; Jiang, S. Y., Ultra low fouling zwitterionic polymers with a biomimetic adhesive group, Biomaterials, 29, 4592-4597 (2008).)

[00012] Additionally, it has been shown that an electrically conductive polymer-nanocomposite membrane containing carbon nanotubes is highly resistant to biofilm formation when an electrical potential is applied across the membrane. *See* de Lannoy, C.-F.; Jassby, D.; Gloe, K.; Gordon, A. D.; Wiesner, M. R., Aquatic Biofouling Prevention by Electrically Charged Nanocomposite Polymer Thin Film Membranes, Environmental Science & Technology (2013). In embodiments of the invention, zwitterion-functionalized nanotubes could function in a similar way, but without the need for the imposed electrical potential, because the groups have permanent charges.

[00013] In this specification, the inventors examine the transport of water and ions through zwitterion-functionalized carbon nanotube membranes using both atomically-detailed modeling and experimental techniques. Examples of zwitterion groups that can be used include those having the structure: $-COO-(CH_2)_3-N^+(CH_3)_2-(CH_2)_2COO^-$. Non-equilibrium MD simulations can be used to calculate both water and ion transport through idealized membranes and it has been found that addition of two zwitterions per tube end can completely block ion transport in membranes having carbon nanotubes with diameters of 15.6 Å. In accordance with embodiments of the invention, the inventors have synthesized carbon nanotube/polyamide nanocomposite membranes using a procedure that partially aligns the carbon nanotubes within the polyamide layer through flow filtration (Kim, Jinschek, Chen, Sholl, and Marland, 2007). Additionally, the performance of the membranes as a function of the concentration of the carbon nanotubes has been measured. It has been found that increasing the weight fraction of carbon nanotubes leads to an increase of both water transport and ion rejection, indicating that the zwitterion-functionalized carbon nanotubes are effective at both conducting water and blocking ion transport. Analysis of these simulations shows that the zwitterion moieties lead to the rejection of ionic

species using a gatekeeper mechanism, involving both steric effects and charge repulsion. Since resistance to water transport is only at the entrance, this provides a distinct advantage over polymer membranes, which have high tortuosity and resistance to water flow throughout the entire thickness of the membrane. The synthesis methods described herein can also be used for large-scale manufacture of carbon nanotube membranes, in contrast to previous carbon nanotube membrane synthesis methods (Holt *et al.*, 2006; Hinds *et al.*, 2004), which require carbon nanotubes to be grown on a substrate. It is this substrate growth that is not scalable.

[00014] Thus, there is a need in the art for novel membranes with both high salt rejection and water transport that are also resistance to biofouling, whose method of fabrication can be scaled to industrial levels.

SUMMARY OF THE INVENTION

[00015] It is thus an objective of the invention to provide a method for fabricating membranes that may be useful for desalination and other filtering applications due to properties such as high salt rejection and water transport and resistance to biofouling.

[00016] It is another objective of the invention to provide a method for fabricating such membranes that may be scaled up to industrial levels.

[00017] Another objective includes providing a membrane that may be useful for desalination and other filtering applications as a result of these methods.

[00018] To achieve the above objectives, the present invention provides methods of fabricating a functionalized carbon nanotube nanocomposite membrane. The carbon nanotubes may be functionalized with zwitterions, or other functional groups, to block transport of ions through the carbon nanotubes while allowing the passage of water molecules.

[00019] In one embodiment, the invention provides a method of fabricating functionalized carbon nanotube nanocomposite membranes, comprising carbon nanotube functionalization, wherein carbon nanotubes are functionalized with

zwitterionic functional groups; deposition, wherein said functionalized carbon nanotubes are deposited on a membrane support; and polymerization, wherein a polymer matrix is deposited over, on, around, and/or in operable communication with, the membrane support and deposited functionalized carbon nanotubes; wherein the zwitterionic functional groups consist of less than 18 carbon atoms and the polymer is polyamide.

[00020] In one aspect of this embodiment, the carbon nanotubes may be single-walled nanotubes.

[00021] In other aspects of this embodiment, the zwitterionic functional groups may consist of less than 16 carbon atoms, less than 14 carbon atoms, less than 12 carbon atoms, less than 10 carbon atoms, less than 8 carbon atoms, or less than 6 carbon atoms.

[00022] In another embodiment, the invention provides a method of carbon nanotube functionalization comprising: a reflux step, wherein carbon nanotubes are refluxed in a combination of sulfuric acid and nitric acid; a thionyl chloride addition step; a 3-(dimethylamino)propan-1-ol addition step; and a β-propiolactone addition step.

[00023] In another embodiment, the invention provides a method of deposition of carbon nanotubes on a membrane support comprising: pretreatment of said membrane support with a surfactant; and filtration of a solution of said carbon nanotubes through said membrane support.

[00024] In another embodiment, the invention provides a method of intrafacial polymerization of polyamide on a membrane support, wherein the membrane support comprises a polyester side and polysulfone side, comprising: contacting the polyester side of the said membrane support with an aqueous solution comprising a diamine; removing said aqueous solution from said membrane support; and contacting the polysulfone side of said membrane support with an organic solution comprising an acid chloride.

[00025] In another embodiment, the invention provides a functionalized

carbon nanotube nanocomposite membrane, comprising a membrane support; carbon nanotubes functionalized with zwitterionic functional groups deposited on the membrane support; and a polymer matrix overlaying the carbon nanotubes and membrane support; wherein the zwitterionic functional groups consist of less than 18 carbon atoms and the polymer is polyamide.

[00026] Various aspects of the aforementioned embodiments will be described in the Detailed Description below.

BRIEF DESCRIPTION OF THE DRAWINGS

[00027] FIG. 1 is a schematic diagram showing an exemplary embodiment of a carbon nanotube functionalization method according to the invention.

[00028] FIG. 2A is a photo showing an exemplary embodiment of a filtration cell for use in a method according to the invention.

[00029] FIG. 2B is a photo showing a polyethersulfone (PES) support membrane with carbon nanotubes deposited using a high-pressure filtration technique according to the invention.

[00030] FIGS. 3A-C are schematic diagrams depicting an exemplary method according to embodiments of the invention for fabricating a carbon nanotube nanocomposite membrane according to the invention.

[00031] FIG. 3D is a photo showing the top of a functionalized carbon nanotube nanocomposite membrane prepared in accordance with embodiments of the method illustrated in FIGS. 3A-C.

[00032] FIG. 4 is a table illustrating different gas permeabilities of non-limiting examples of carbon nanotube nanocomposite membranes according to the invention.

[00033] FIG. 5A is a table illustrating water flow and salt rejection of a non-limiting example of a carbon nanotube nanocomposite membrane according to embodiments of the invention.

[00034] FIG. 5B is a graph illustrating water flow and salt rejection of a non-

limiting example of a carbon nanotube nanocomposite membrane according to embodiments of the invention.

[00035] FIG. 6 is a computer rendered image depicting a simulation setup for simulation studies of nanotubes to model the effects of water and ion transport through functionalized single-wall nanotube membranes.

[00036] FIG. 7A is a graph illustrating a computer simulation of the flux of salt ions through a pristine single-walled carbon nanotube membrane.

[00037] FIG. 7B is a graph illustrating a computer simulation of the flux of salt ions through a single-walled carbon nanotube functionalized with two zwitterions on the end of each nanotube.

[00038] FIG. 8 is a computer rendered image depicting a simulation cell containing a membrane composed of four carbon nanotubes embedded between two graphene sheets with saltwater on either side of the membrane, wherein each end of the tube is functionalized with two zwitterionic groups.

[00039] FIGS. 9A and 9B are graphs illustrating conductance of water and ions, respectively, as a function of simulation time per carbon nanotube (20,0) for pristine (non-functionalized) nanotubes, carbon nanotubes with one zwitterion at each end, and with two zwitterions at each end for a bulk concentration of 0.6 M NaCl and a pressure drop of 208 MPa.

[00040] FIGS. 10A and 10B are graphs illustrating conductance of water and ions, respectively, as a function of simulation time per carbon nanotube (26,0) for carbon nanotubes with two zwitterions at each end, with four zwitterions at each end, and with five zwitterions for each end for a bulk concentration of 0.6 M NaCl and a pressure drop of 208 MPa.

[00041] FIG. 11 is a graph illustrating water flux and salt rejection ratio as a function of carbon nanotube concentration in the selective polyamide layer of a non-limiting example of a nanocomposite membrane of the invention.

[00042] FIGS. 12A and 12B are graphs illustrating conductance of water and ions, respectively, as a function of simulation time through carbon nanotubes

functionalized with one or two zwitterions per tube end and with charges on the zwitterions turned on or off.

[00043] FIG. 13A-C are schematic diagrams illustrating configurations of zwitterions that are extended (unfolded) into the liquid phase or folded inside the carbon nanotube for a (20,0) system with (A) one zwitterion or (B) two zwitterions per tube end and for a (26,0) system with (C) five zwitterions per tube end.

[00044] FIGS. 13D and 13E are PMF diagrams illustrating free energy as a function of carbon position along the z axis, wherein FIG. 13D is a PMF diagram for moving one zwitterion in a (20,0) carbon nanotube with one or two zwitterions per tube end, and FIG. 13E is a PMF diagram for moving one zwitterion in a (26,0) carbon nanotube with two or five zwitterions per tube end.

[00045] FIG. 14 is a table illustrating water and ion flow rate (number per ns per carbon nanotubule) and ion rejection ratio as a function of salt concentration for flow through a (20,0) carbon nanotubule having one zwitterion functional group at each end.

[00046] FIG. 15 is a graph illustrating salt rejection of NaCl feed concentration for a plain polyamide membrane and a non-limiting example of a nanocomposite membrane with 20 wt% carbon nanotubes.

[00047] FIGS. 16A and 16B are graphs illustrating conductance of water and ions, respectively, per carbon nanotube as a function of simulation time for pristine non-functionalized nanotubes, carbon nanotubes with one zwitterion at each end and with two zwitterions at each end for a bulk concentration of 0.6M KCl and a pressure drop of 208 MPa.

[00048] FIGS. 17A-C are graphs illustrating water flux and salt rejection for a pure polyamide membrane, 9wt% zwitterion-functionalized single-walled nanotube/polyamide nanocomposite membrane and a 20 wt% zwitterions-functionalized single-walled nanotube/polyamide nanocomposite membrane operated for a pressure drop of 530 psi.

[00049] FIGS. 18A-C are field emission scanning microscopy images of

surface morphologies of a (FIG. 18A) PES support, (FIG. 18B) plain polyamide membrane, and (FIG. 18C) zwitterion-functionalized carbon nanotube/polyamide nanocomposite membrane.

[00050] FIG. 18D is a field emission scanning microscopy image of a cross-sectional view of a zwitterion-functionalized carbon nanotube/polyamide nanocomposite membrane.

DETAILED DESCRIPTION OF EXEMPLARY EMBODIMENTS OF THE INVENTION

[00051] Reference will now be made to various figures showing exemplary embodiments of the invention. However, the embodiments described in the description and shown in the figures are illustrative only and are not intended to limit the scope of the invention, and changes may be made in the specific configurations and materials described in this specification and accompanying drawings that a person of ordinary skill in the art will recognize are within the scope and spirit of the invention.

[00052] In this specification, the following abbreviations may be used and may be defined further in other parts of the specification: SWNT, single-walled nanotubes, PES, polyethersulfone, TMC, trimesoyl chloride, MPD, m-phenylene diamine, and TFN, thin film nanocomposite. Other common abbreviations will be apparent to a skilled artisan.

[00053] In accordance with embodiments of the invention, a method of the present invention may comprise a procedure or process for fabrication of a functionalized carbon nanotube nanocomposite membrane. The method may comprise a carbon nanotube functionalization step, wherein carbon nanotubes are functionalized with zwitterions or other functional groups, a deposition step, wherein said functionalized carbon nanotubes are deposited on a membrane support, and a polymerization step, wherein a polymer matrix is deposited over the membrane support and/or carbon nanotubes to create a functionalized carbon nanotube nanocomposite membrane. A product or products of the present invention may comprise functionalized carbon nanotube nanocomposite

membranes fabricated by such a method. The membranes of the present invention possess a number of potential advantages over the prior art, only some of which that are discussed herein, including high water flux, excellent salt rejection, and resistance to biofouling. The membranes of the present invention, and the method of their fabrication, may be particularly beneficial for use in desalination, water purification, and gas separation.

[00054] In accordance with embodiments of the present invention, carbon nanotubes, nanotubes for use in nanocomposite membranes and for use in membrane fabrication methods of the invention may have a pore diameter of about 0.1 nm to about 50 nm, 0.1 nm to about 10 nm, such as from about 0.1 nm to about 3.0 nm, about 0.4 nm to about 2.5 nm, about 0.4 nm to about 2.0 nm, about 0.6 nm to about 1.8 nm, about 0.6 nm to about 1.5 nm, about 0.6 nm to about 1.3 nm, about 0.6 nm to about 1.1 nm, about 0.4 nm to about 1.1 nm, about 0.4 .to about 0.9 nm, about 0.8 nm to about 1.1 nm, about 0.7 nm to about 1.2 nm, about 0.9 nm to about 1.1 nm, and so on.

[00055] Carbon nanotubes, nanotubes for use in nanocomposite membranes, and for use in membrane fabrication methods of the invention may have a pore diameter of about 1 Å to about 100 Å, about 2 Å to about 30 Å, about 5 Å to about 25 Å, about 10 Å to about 20 Å, about 10 Å to about 18 Å, about 10 Å to about 16 Å, about 10 Å to about 14 Å, about 10 Å to about 12 Å, about 12 Å to about 20 Å, about 14 Å to about 24 Å, about 16 Å to about 22 Å, about 12 Å to about 18 Å, about 14 Å to about 16 Å, about 15 Å to about 19 Å, about 11 Å to about 15 Å, and so on.

[00056] Further, carbon nanotubes, nanotubes for use in nanocomposite membranes, and for use in membrane fabrication methods of the invention may have a length anywhere from about 0.1 μm to about 10 μm, about 0.1 μm to about 2.0 μm , about 0.5 μm to about 1.5 μm, about 0.7 μm to about 1.3 μm, about 0.8 μm to about 1.2 μm , about 0.9 μm to about 1.1 μm , about 0.5 μm to about 1.2 μm, about 0.9 μm to about 1.5 μm, about 0.8 μm to about 1.4 μm , about 0.7 μm to about 1.1 μm, and so on.

[00057] Such carbon nanotubes may have a length anywhere from about 20 Å to about 100 Å, about 30 Å to about 50 Å, about 35 Å to about 45 Å, about 36 Å to about 44 Å, about 37 Å to about 43 Å, about 38 Å to about 42 Å, about 40 Å to about 44 Å, about 41 Å to about 43 Å, about 39 Å to about 42 Å, about 41 Å to about 45 Å, about 40 Å to about 42 Å, about 42 Å to about 44 Å, and so on.

[00058] The length, diameter, and other properties of the carbon nanotubes may be chosen according to the particular filtering applications desired for the nanocomposite membrane. For example, for gas separations, smaller pore diameters which selectively allow specific gas molecules to pass through the nanocomposite membrane while excluding other gas molecules may be used, while for desalination applications, pore sizes which allow water molecules to pass through the nanocomposite membrane while excluding salt ions may be used. Further, the length of the nanotubes may be chosen according to the thickness of the membrane desired.

[00059] The methods of the present invention may use a variety of types of carbon nanotubes, including multi-walled carbon nanotubes (MWNTs), double-walled carbon nanotubes (DWNTs), and single-walled carbon nanotubes (SWNTs). In a preferred embodiment, single-walled nanotubes (SWNTs) are used. The carbon nanotubes may be synthesized through a variety of methods known in the art, including arc discharge, laser ablation, plasma torch, high pressure CO disproportion, and chemical vapor deposition (CVD). In a preferred embodiment, CVD is used to produce the carbon nanotubes.

[00060] SWNTs for use in methods of the invention may be of a variety of dimensions such as those disclosed herein. A non-limiting example of a SWNT for use in nanocomposite membranes of the invention is a SWNT with an outer diameter of 1.5 nm and a length of 1 μm. Another non-limiting example of a SWNT for use in nanocomposite membranes of the invention is a SWNT with a diameter of about 15.6 Å and a length about 41.2 Å. Another non-limiting example of a SWNT for use in nanocomposite membranes of the invention is a SWNT with a diameter of about 20.3 Å and a length of about 43.3 Å. In other

embodiments, SWNTs for use in membrane fabrication have an outer diameter of about 0.5 nm to about 2.0 nm, and a length anywhere from about 0.1 μm to 10 μm, and any range in between such as those disclosed herein. Indeed, any of the specific ranges disclosed above for length, pore size/diameter, and whether the structure is single walled, double walled, or multi-walled can be combined in any manner to obtain nanotubes according to the invention.

[00061] In various embodiments of methods according to the invention, the carbon nanotubes can be functionalized with a variety of functional groups, including but not limited to alkanes, alkenes, alkynes, phenyl groups, alkyl halides, amines, amides, alcohols, ethers, aldehydes, ketones, carboxylic acids, ethers, esters, nitrates, nitrites, alkoxy groups, hydroxyl groups, amino groups, halo groups, carbonyl groups, benzyl groups, cyano group, silyl groups, sulfonic acid groups, phosphoric acid groups, boronic acid groups, free radicals, and any combination thereof. Preferred are functional groups that are sufficiently bulky to provide steric hindrance and sufficiently charged to provide electrostatic repulsion for exclusion of ions, as well as of a high dipole movement. In a preferred embodiment, the carbon nanotubes are functionalized with zwitterion functional groups. Preferred are short zwitterion functional groups such as those with less than 18 carbon atoms, more preferably less than 16 carbon atoms, still more preferably less than 14 carbon atoms, still more preferably less than 12 carbon atoms, still more preferably less than 10 carbon atoms, still more preferably less than 8 carbon atoms, and most preferably less than 6 carbon atoms. Even more preferred are short zwitterion functional groups having 5 carbon atoms. Still more preferred are zwitterion functional groups with the structure: $-COO-(CH_2)_3-N^+(CH_3)_2-(CH_2)_2COO^-$. However, other structures may be substituted. Indeed, any functional group comprising from 1-20 carbon atoms can be used and including other atoms such as oxygen, nitrogen, sulfur, and/or halogens. These include zwitterion functional groups wherein the positive and negative charges are located at different locations.

[00062] In a particular embodiment of a carbon nanotube functionalization

procedure, SWNTs are obtained as starting material and then purified and functionalized with COOH groups by refluxing in sulfuric acid/nitric acid. Through this method, it is contemplated that purity of the SWNTs may be greater than 95% (by TGA) and concentration of COOH groups in the SWNTs may be approximately 2-7 wt% (by titration). However, variations of this procedure and other methods of functionalization of SWNTs with COOH groups may be used.

[00063] In accordance with methods of the invention, the COOH groups in the SWNTs may serve as precursors for the addition of short zwitterion groups. FIG.1 shows an exemplary embodiment of a series of chemical reactions for converting COOH groups to zwitterion groups. The series of reactions produce a series of chemical modifications and may include a thionyl chloride addition step, a 3-(dimethylamino)propan-1-ol addition step, and a β-propiolactone addition step. In particular, in the first step, COOH functionalized SWNTs may be reacted with thionyl chloride to change COOH groups into COCl groups (FIG 1(A)). The experimental procedure followed to make this conversion was reported by Jain et. al. Acyl chloride functionalized SWNTs may then be reacted with 3-(dimethylamino)propan-1-ol to form the compound shown in FIG 1(B), which may then be reacted with β-propiolactone to form the compound shown in FIG 1(C) (the zwitterion-functionalized SWNTs).

[00064] After each chemical modification, further purification and extraction methods may be utilized to purify the modified carbon nanotubes and to remove unreacted reagents. These purification and extraction methods may involve washing the carbon nanotubes in a suitable solvent, centrifugation, filtration, and/or drying.

[00065] For example, in a non-limiting, exemplary procedure for converting acyl chloride-functionalized SWNTs to zwitterion-functionalized SWNTs, 100 mg of COCl SWNTs (0.1 mmol of COCl group) may be added to a mixture of 1.2 ml 3-(dimethylamino)propan-1-ol (10 mmol) and 1.4 ml of triethyl amine (10 mmol) in a 100 ml flask. The reaction mixture may be stirred for 6 days at 100 RPM and room temperature. The SWNTs may then be washed with ethanol to remove

ethylamine hydrochloride salt and dried under vacuum. In the third step, SWNTs may be reacted with β-propiolactone to form zwitterion-functionalized SWNTs. Further, 100 mg of functionalized SWNTs may be added to 20 ml of dry tetrahydrofuran (THF) in a 50 ml flask. The reaction mixture may be stirred under nitrogen protection at room temperature for 5 hours. SWNTs may be washed with dry THF and separated by centrifuging. They may be dried under vacuum to remove any washing solvent. The zwitterion functional group is circled red in FIG. 1(C). The amounts of reagents described herein are merely exemplary, and differing amounts and ratios may be substituted as appropriate as may be appreciated by a skilled artisan

[00066] The methods to functionalize COOH carbon nanotubes with zwitterion groups taught in this disclosure have not been previously described in the art. These zwitterion groups have a variety of advantages according to the invention including a very high dipole moment, which helps in creating a strong hydration layer near the feed surface of the membrane, eliminating the biofouling of the membrane. The zwitterion-functionalized SWNTs may be used in the separation layer of the thin film nanocomposite membrane, thus making biofouling free desalination membranes. However, other procedures for attaching zwitterions to carbon nanotubes may be used. For example, various amino acids or small peptides in zwitterionic form, or their derivatives could be substituted, and chemically attached to the carbon nanotubes, instead of the procedure shown in FIG. 1.

[00067] Various embodiments of carbon nanotubes for use in methods for fabricating functionalized carbon nanotube nanocomposite membranes according to embodiments of the invention may include a range of a number of functional groups attached to carbon nanotubes. For example, for zwitterionic groups, various embodiments include carbon nanotubes with anywhere from 1 zwitterion to 20 zwitterions attached at one or both ends. Other embodiments include carbon nanotubes with 1 zwitterion to 10 zwitterions attached at one or each end, or from 1 zwitterion to 5 zwitterions attached at one or each end, or

foam 2 zwitterions to 6 zwitterions attached at one or each end, or from 1 zwitterion to 3 zwitterions attached at one or each end, or from 2 zwitterions to 5 zwitterions attached at one or each end, 4 zwitterions to 7 zwitterions attached at one or each end, 1 zwitterion to 2 zwitterions attached at one or each end, or from 7 zwitterions to 10 zwitterions attached at one or each end, 5 zwitterions to 9 zwitterions attached at one or each end, 3 zwitterions to 5 zwitterions attached at one or each end, 2 zwitterions to 4 zwitterions attached at one or each end, and so on. Other embodiments include similar ranges of zwitterions attached at one end only, or attached on the inside of the carbon nanotubes. For example, for nanotube embodiments comprising 4 zwitterions to 7 zwitterions attached at one or each end, the nanotubes can comprise 4, 5, 6, or 7 zwitterions attached at one end, or 4 zwitterions attached at each end or only at one end, or 4 zwitterions attached at one end and 5, 6, or 7 zwitterions attached at the other end, or 5 zwitterions attached at one end and 4, 6, or 7 zwitterions attached at the other end, or 6 zwitterions attached at one end and 4, 5, or 7 zwitterions attached at the other end, or 7 zwitterions attached at one end and 4, 5, or 6 zwitterions attached at the other end, and so on.

[00068] In accordance with methods of the invention, after the carbon nanotubes are modified with functional groups, the carbon nanotubes may be deposited on a membrane support. To accomplish deposition, a dispersion of the carbon nanotubes may be made. The deposition of functionalized carbon nanotubes on a membrane support may include pretreatment of the membrane support with a surfactant and filtration of the dispersion through the support to deposit the carbon nanotubes.

[00069] In certain embodiments of methods according to the invention, the dispersion of carbon nanotubes may be made in a variety of solvents or surfactants. Use of various solvents or surfactants that allow for efficient dispersion and alignment of the carbon nanotubes is contemplated. If a solvent is used, various concentrations of the carbon nanotubes in the solvent are contemplated. In certain embodiments of the invention, the solvent may be water.

In other embodiments, other solvents that may be used for dispersion of the carbon nanotubes may be chosen from tetrahydrofuran (THF) 1,4-dioxane, acetone, acetonitrile dimethylfornamide, dimethylsulfoxide, or the like. However, there may be other solvents more suitable for dispersion of the carbon nanotubes, depending on the type of chemical functional group that may be present on the carbon nanotubes. For example, if a hydrophobic functional group has been added to the carbon nanotubes, it may be more desirable to disperse the carbon nanotubes in a non-polar solvent such as diethylether, hexane, benzene, toluene, chloroform, ethyl acetate, dichloromethane or the like.

[00070] In certain embodiments of methods according to the invention, the membrane support may be made of a variety of materials, including polyfluoroethylene (PTFE) and polyvinylidene fluoride (PVDF), or hydrophilic materials, such as polypropylene, polyethersulfone (PES), and nylon.

[00071] In certain embodiments of methods according to the invention, the surfactant may be an anionic surfactant such as sulfate, sulfonate, and phosphate esters, including but not limited to sodium dodecylsulfonate, sodium dodecylbenzenesulfonate, ammonium lauryl sulfate, sodium laureth sulfate, alkyl benzene sulfonate, and the like.

[00072] In certain embodiments of methods according to the invention, the dispersion may be filtered through the membrane support through high-pressure filtration or vacuum filtration, or at ambient pressure, atmospheric pressure, or no pressure.

[00073] For example, in a non-limiting example of a procedure for depositing functionalized SWNTs on a membrane support, a fixed amount of zwitterion-functionalized SWNTs, depending on the desired concentration of SWNTs in the membrane, may be sonicated in deionized water, in a volume, for example, of 40 ml, to create a carbon nanotube solution. Polyethersulfone (PES) membrane supports may be pretreated by soaking in a surfactant solution. For example, a surfactant solution of sodium dodecylbenzenesulfonate at a concentration of 0.5% (w/v) may be used. The surfactant treatment may be of

various lengths of time, ranging from 1 hour, to several hours, up to 1 day or even up to 1 week. In a preferred embodiment, the membrane supports are pretreated for two days. Not wishing to be bound by theory, surfactant pretreatments may make the membrane support more hydrophilic and also at the same time open the pores of the support enabling to filter the carbon nanotube dispersion through it using an apparatus shown in FIG. 2A, which shows a Millipore filtration cell. The length of time of pretreatment may be adjusted according to the strength and concentration of surfactant used. In another embodiment, after soaking in the surfactant solution, the PES support may be stored in deionized water to remove any excess of surfactant. The PES support may be stored in water for at least four hours up to and including 72 hours, for example. In a preferred embodiment, the PES support is stored in water for one day. The SWNTs may then deposited on the membrane support using various techniques, such as high-pressure or vacuum filtration method, or gravity, wherein the support acts as a filter paper and the carbon nanotubes are filtered out of the solution and aligned on the support.

[00074] In further accordance with a non-limiting example of a procedure for depositing functionalized SWNTs on a membrane support, the membrane support may be fitted at the bottom of the filtration cell, and filled with carbon nanotube dispersion and pressurized using an inert gas such as nitrogen at high pressure (at least 40 PSI feed gas tank pressure). The dispersion inside the filtration cell may be stirred at a very low RPM (for example, around 50). The stirring helps in forming a uniform layer of SWNTs on top of the PES support as shown in FIG. 2B, which shows the polyethersulfone (PES) support membrane with functionalized carbon nanotubes deposited using the high-pressure filtration technique described here. Alternatively, the carbon nanotubes may be deposited by other filtration techniques such as vacuum filtration.

[00075] The inventors filed a patent application on alignment of SWNTs using high-pressure filtration technique. This patent, U.S. Patent No. 7,931,838, which is incorporated by reference herein in its entirety, discloses alignment and

deposition of functionalized carbon nanotubes on one or more membrane support material using high-pressure filtration and a unique filtration cell. Deposition of carbon nanotubes on PES supports using high pressure filtration to make thin film nanocomposite membranes (TFN) for desalination have not been previously taught in the art. According to the invention, this technique has the added advantage of controlling the concentration of the functionalized SWNTs in the separation layer of the polyamide-carbon nanotube TFN membrane. This control can be achieved by making the carbon nanotube dispersion of desired weight percentage, which is filtered through the support.

[00076] For example, zwitterion-functionalized carbon nanotube nanocomposite membranes of the invention may be fabricated with zwitterion-functionalized carbon nanotubes at weight percentages in the polymer layer ranging from about 0.1 wt% to about 99.9 wt%, 10 wt% to about 90 wt%, 40 wt% to about 80 wt%, 60 wt% to about 70 wt%, such as from about 1 wt% to about 50 wt%, 1 wt% to about 20 wt%, 2 wt% to about 20 wt%, or from about 5 wt% to about 30 wt%, 10 wt% to about 30 wt%, 15 wt% to about 25 wt%, or from about 16 wt% to about 24 wt%, 18 wt% to about 26 wt%, 18 wt% to about 25 wt%, 15 wt% to about 23 wt%, 19 wt% to about 21 wt%, 18 wt% to about 22 wt%, 17 wt% to about 23 wt%, and so on. The particular concentration of carbon nanotubes may be selected based on various factors including the functional groups attached to the carbon nanotubes, dimensions of the carbon nanotubes, and the number of functional groups attached. Any combination of one or more of these features, especially combinations of the particular dimensions provided in this specification for these features, can be used to obtain a desired nanotube according to the invention. Non-limiting examples of proportions of zwitterion-functionalized carbon nanotubes making up a composite membrane include 9 wt% and 20 wt% of the polymer matrix. In embodiments, the polymer matrix comprises polymer and nanotubes to provide a matrix.

[00077] In accordance with methods of the invention, after carbon nanotubes are deposited on a membrane support, a polymerization step, wherein

a polymer matrix is deposited over the membrane support and deposited functionalized carbon nanotubes to create a functionalized carbon nanotube nanocomposite membrane, may be included to complete fabrication. Preferred is the interfacial polymerization procedure described below.

[00078] In certain embodiments of methods according to the invention, intrafacial polymerization may occur through contact of an organic solution comprising an acid chloride with an aqueous solution comprising a diamine. In particular embodiments, the organic solution comprises trimesoyl chloride (TMC) and the aqueous solution comprises phenylene diamine (MPD).

[00079] In certain embodiments of methods according to the invention, the organic solution and aqueous solution are introduced on different sides of the support. For example, in one embodiment, wherein the membrane support is a PES support comprising a polysulfone side and a polyester side, the organic solution may be introduced on the polysulfone side of the support and the aqueous solution may be introduced on the polyester side of the support. However, in other embodiments, the organic solution may be introduced on the polyester side of the support and the aqueous solution may be introduced on the polysulfone side of the support.

[00080] In embodiments, the aqueous solution contains a surfactant and the organic solution contains a non-polar solvent.

[00081] Also in embodiments, the organic solution and the aqueous solution may be briefly introduced to the membrane support as described above, and then removed. The membrane support may then be cured at high temperature and then washed to remove excess solution.

[00082] For example, in a non-limiting example of an interfacial polymerization protocol according to the invention, after filtering the carbon nanotube dispersion through the PES support, the support may be dried in a vacuum oven (for example, for one hour). It may then be soaked in 0.5 % (w/v) surfactant solution (for example, for one day). To carry out interfacial

polymerization, two solutions, an aqueous and an organic solution may be prepared. The aqueous solution and the organic solution contain m-phenylene diamine (MPD) and trimesoyl chloride (TMC), respectively. The MPD solution contains surfactant along with the MPD. In one example, the concentration of surfactant may be 0.2 % (w/v) and the concentration of MPD may be 2 % (w/v) in water. The concentration of TMC may be 0.5 % (w/v) in hexane or similar organic solvent. However, differing concentrations within this general range may be used, such as any of one or more of the surfactant, the MPD, and/or the TMC being present in a range of from about 0.1 % (w/v) to about 20 % (w/v), such as from about 0.3 % (w/v) to about 7 % (w/v), such as from about 0.4 % (w/v) to about 4 % (w/v), or from about 0.6 % (w/v) to about 3 % (w/v), or from about 0.7 % (w/v) to about 1 % (w/v), and so on.

[00083] In further accordance with a non-limiting example of a interfacial polymerization protocol according to the invention, the PES support with the deposited carbon nanotubes may be placed between two circular PTFE frames, holding together using a metal clamp. The interfacial polymerization method followed here is different from the one generally described in the art. This method of interfacial polymerization may be referred to herein as 'Back and Front' interfacial polymerization method. In this method, the polyester side of the PES support may be briefly soaked with MPD (for example, 1 min). The MPD solution may be drained and the support dried for a minute, cleaning the excess MPD solution using a Kim wipe or other suitable absorbent material. Then, the TMC solution may be briefly introduced (for example, 2 minutes) on the polysulfone side of the support, using a syringe, pipet, or other suitable transfer means and then may be drained. Polymerization will occur relatively quickly (within minutes). The TFN membrane prepared may be cured in air-circulated oven briefly at high temperature (for example, at 68°C for 5 min). The membrane may be washed in DI water to remove excess MPD, and then stored in water for at least one day before testing for either gas separation or desalination. In another embodiment, the interfacial polymerization could be

carried out by briefly soaking the front side with MPD solution (for example, for about 2 min). The excess solution from the impregnated membrane may then be removed using a glass roller or other suitable means. The membrane may be placed back to the PTFE frame and the TMC solution may be introduced on the front side of the support using a syringe or pipet. The TMC solution may be drained very slowly after a brief period (for example, 90 seconds) and the following procedures were identical to that mentioned previously.

[00084] The 'Back and Front (B-F)' intrafacial polymerization (IP) method is particularly advantageous over prior art intrafacial polymerization methods, where both the MPD and the TMC solutions are introduced on the polysulfone side of the membrane followed in making desalination membranes. Intrafacial polymerization methods previously described in the art result in a loose polyamide layer formed on the top of the SWNTs. This layer was washed away while testing the membranes for desalination. However, by following the Back and Front intrafacial polymerization method described herein in forming polyamide embedding the functionalized carbon nanotubes over the PES support, the polyamide formed adhered to the polysulfone thereby forming an excellent integral membrane. This was confirmed through scanning electron microscopy (SEM) images of the cross-section of the membranes prepared by both methods. While testing for salt rejection, the polyamide layer did not get washed away, and showed good water flux with a significant salt rejection. The novel 'Back and Front' intrafacial polymerization method described herein has proved to be very critical in the possibility of making an integral thin film nanocomposite membrane exhibiting excellent desalination properties.

[00085] Additionally, various embodiments of methods of fabricating functionalized carbon nanotube nanocomposite membranes according to the invention include use of a range of materials for forming the polymer of the nanocomposite. While polyamide is preferred, particularly according to the intrafacial polymerization methods described herein, other polymers commonly used in desalination membranes may be substituted in the methods disclosed

herein, including polyurea, polyimide, polycarbonate, polymethacrylate, polysulphone, other thermoplastic polymers, or cellulosic polymers (e.g., cellulose acetate (CA) and cellulose triacetate (CTA)). Various methods of polymerization of these materials are known in the art.

[00086] FIGS. 3A-D together provide an overview of a non-limiting example of a method for fabricating carbon nanotube nanocomposite membranes according to the invention. FIG. 3A represents a PES ultrafiltration membrane, composed of a thin PES layer covered on a nonwoven polyester web, soaked in a surfactant solution to clean the pores and increase hydrophilicity. The membrane was then sandwiched by two PTFE holders. FIG. 3B represents zwitterion-functionalized carbon nanotubes, deposited on the pretreated PES membrane, through vacuum filtration. FIG. 3C represents interfacial polymerization of polyamide carried out between semi-aligned functionalized carbon nanotubes at which aqueous solution of MPD comes in contact with the non-aqueous solution of TMC. FIG. 3D shows a photograph of the top of the functionalized carbon nanotube nanocomposite membrane that is exposed to the feed. Overall, the methods according to the invention detailed in this disclosure have not been previously described in the art. In particular, the excellent control on the concentration of the carbon nanotubes in the separation layer, and the functional group on the carbon nanotubes, especially zwitterion functional groups makes possible the fabrication of high water flux membranes with excellent salt rejection without biofouling.

[00087] Embodiments of the invention include methods of fabricating functionalized carbon nanotube nanocomposite membranes scaled up to industrialized scales for industrial membrane manufacture. For example, some of the individual steps may be carried out in industrial reactors wherein raw material or materials enter a reactor to produce a product. The product may be an intermediate product that is subsequently feed to a second downstream reactor, which is fed additional raw material or materials to produce a second intermediate product, which is then fed to a third downstream reactor, which is

fed additional raw material or materials to produce a third intermediate product, and so on. Alternatively, intermediate products may be fed on a conveyor to different stations where individual fabrication steps occur, either through automation, human assistance, or a combination of both. For example, in one embodiment of an industrial membrane manufacturing process, interfacial polymerization of polyamide is carried out by industrial sprayers that apply the MPD and TMC solutions to a PES membrane that has previously been applied zwitterion-functionalized carbon nanotubes at an upstream processing station. Scaling of the fabrication steps disclosed herein to an industrial scale is within the capabilities of a skilled chemical engineer or industrial chemist.

[00088] The present invention also provides various embodiments of functionalized carbon nanotube nanocomposite membranes, including those fabricated by the methods described herein. The functionalized carbon nanotube nanocomposite membranes may comprise any component at any specification in any range disclosed above, such as with respect to the types of carbon nanotubes, carbon nanotube length and pore diameter, functional group type, structure, length, number, and position, type of polymer, and weight percentage of the carbon nanotubes in the polymer layer.

[00089] After the nanocomposite membranes are formed, they may be used as is for filtration or further modified. It is contemplated that additional modifications may be made to the nanocomposite membranes to confer additional properties. For example, additional layers of polymers may be added to the nanocomposite membranes in order to modify their permeability. It is contemplated that chemical modifications may be made to the carbon nanotubes, polymer, or membrane support to change the properties of the membrane.

[00090] As further described in the Examples below, the nanocomposite membranes of the invention exhibit excellent properties for filtration applications including high water flux, excellent salt rejection, resistance to biofouling, and high gas permeability and selectivity. The functionalized carbon nanotube nanocomposite membranes of the invention have a variety of applications, only

some of which are discussed herein. They may be used as membranes in desalinization plants for reverse-osmosis filtration of salt water, and are durable enough for use in conjunction with high pressure pumps. Since the membranes of the invention are resistant to biofouling, this obviates the use of biocides and biofouling inhibitors in desalination plants that employ them. Further, the membranes may be used for other water filtering and purification applications, such as removal or harmful waterborne pathogens such as *Cryptosporidium* and *Giardia* as well as toxins such as perchlorate, and may be used for water purification at utilities, at households, or campsites. In addition, the membranes of the invention can be used to separate various gases in mixtures that result from industrial processes, such as chemical plants, oil refineries, gasification plants, etc. Additional applications that are contemplated include the use in respirators, drug delivery channels for drug delivery, chemical sensing, and protein purification. Additional, non-limiting descriptions of some of the properties and advantages of the nanocomposite membranes according to the invention will be provided in the Examples below.

[00091] EXAMPLES

[00092] Embodiments of membranes according to the invention were tested in various applications. FIG. 4 shows results of gas permeabilities of nanocomposite membranes according to the invention that have differing amounts of zwitterion-functionalized carbon nanotubes in comparison to a pure polyamide membrane. Gas permeabilities of all the gases tested increased with increase in the concentration of the carbon nanotubes without affecting the selectivity. For 5 mg zwitterion(z)-carbon nanotube polyamide membrane, the permeability increased by a factor of 11 (H_2), 19 (N_2), 33 (O_2), 20 (CH_4) and 37 (CO_2) compared to the pure polyamide membrane. The functional group in the carbon nanotubes also affected (increased) the gas permeabilities, but not the selectivities. For same concentration (1 mg carbon nanotube) polyamide membranes, COOH functionalized carbon nanotube membrane showed higher permeabilities compared to the zwitterion-functionalized carbon nanotube

membrane. This is in accordance with the sorption results obtained for the COOH and zwitterion-functionalized carbon nanotubes.

[00093] By embedding functionalized carbon nanotubules into the separation layer of a thin polyamide composite membrane, the permeability was enhanced tremendously without sacrificing the selectivity of the pure polyamide membrane. Therefore, in other embodiments based on the choice of (i) the monomers for interfacial polymerization (ii) diameter and (iii) functional group of carbon nanotubules, thin nanocomposite membranes may be fabricated whose gas separation performance (high permeability and selectivity) transcends Robeson upper bound, and consequently make these membranes economically attractive for gas separation operations in a chemical plant.

[00094] FIGS. 5A and 5B show results obtained from a reverse osmosis testing of zwitterion-functionalized carbon nanotube nanocomposite membranes with 0.25 mg of carbon nanotube. The table in FIG. 5A compares the water flux (unit in GFD) and salt rejection (unit in %) within three consecutive testing days. At 530 psi, there is no significant drop in the salt rejection rate after three days of testing. Testing verified that the membrane is durable and stable against the surface fouling by salt water. For comparison, reverse osmosis membranes consisting of neat polyamide coating of similar thickness (without carbon nanotubes) on the same support had much lower water flux (0 – 7 GFD) and lower rejection rates (less than 57%).

[00095] Simulations were carried out using standard molecular dynamics techniques and tested potential models to model the effects of water and ion transport through functionalized SWNT membranes. Two different types of nanotubes were used in the simulations in order to identify effects due to the diameter of the SWNTS. The tubes used were (17,0), having diameters of 1.33 nm, and (20,0) SWNTs, having diameters of 1.56 nm. The diameter of the (20,0) SWNTs are very close to the average diameter of the nanotubes used in the experiments. The model membrane was constructed by embedding the nanotubes between a pair of graphene sheets that prevented water and ions

from flowing through the space between the nanotubes. One embodiment of a simulation set up is shown in FIG. 6. Various functional groups were affixed to the ends of the SWNTs in the simulations in order to identify effects due to the gate keeper molecules. The simulation tested nanotubes with no functional group (pristine), with carboxylic acid groups, and with zwitterions. The model membrane setup shown in FIG. 6 shows SWNTs (wire cage), water molecules (red and white sticks), Na^+ (blue spheres), Cl^- (green spheres), and zwitterion groups (space filled models at the ends of the nanotubes), as well as two graphene planes (wire frames).

[00096] Flow of water and ions was induced in the simulation by imposing a pressure drop across the membrane and carrying out simulations for 2 million time steps (with a time step of 1 femtosecond). The flux of water, sodium ions (Na^+) and chloride ions (Cl^-) through the model membrane was measured during the course of the simulation. The results are plotted in FIGS. 7A and 7B, which illustrate a computer simulation of the flux of salt ions through a pristine single-walled carbon nanotube membrane and a single-walled carbon nanotube functionalized with two zwitterions on the end of each nanotube. The zwitterions effectively block the salt flux under identical conditions of operation according to the predictions from the simulations. The results of the simulations show that zwitterions can function as gatekeeper molecules to effectively inhibit the flow of salt ions (such as Na^+ and Cl^-) through the nanotube membrane. Simulations under identical conditions for the pristine nanotubes (FIG. 7A) show that the flux of salt ions through the membrane increases linearly with time, and hence the membrane is ineffective at blocking salt transport and would therefore not be effective for use in a desalination membrane. On the other hand, the simulations clearly demonstrate that functionalizing one or both ends of the nanotubes with at least two zwitterion functional groups makes the ion flux drop to almost immeasurable values over the length of the simulation, as shown in FIG. 7B. Hence, the zwitterions are effective gatekeeper moieties that turn an unselective membrane into a highly selective membrane suitable for desalination.

[00097] Water Flux and Ion Rejection. Molecular simulations clearly show that zwitterion-functionalized carbon nanotubes reject ions, while allowing an acceptable flux of water. Another embodiment of a simulation cell for single-walled carbon nanotube membranes is shown in FIG. 8, which depicts a simulation cell containing a membrane composed of four carbon nanotubes embedded between two graphene sheets with saltwater on either side of the membrane, wherein each end of the tube is functionalized with two zwitterionic groups. In FIG. 8, the carbons of the carbon nanotubes and graphene sheets are shown as cyan lines. Water molecules are shown as red and white sticks, Cl^- and Na^+ ions are shown as green and blue spheres, respectively, and the atoms of the zwitterions are shown as space filling models, cyan for C, red for O, white for H, and magenta for N.

[00098] Each end of each tube was functionalized with 0, 1, or 2 zwitterion groups. The diameter of each tube is about 15 Å, which is similar to the average diameter of the carbon nanotubes used in experiments. The conductance of water and ions for NaCl solutions was calculated at a pressure drop of 208 MPa through pristine and functionalized carbon nanotubes. This large pressure drop was used in order to improve the sampling statistics in the simulations, because the time scales accessible in simulations were only on the order of 10s of nanoseconds. We note that extrapolation to lower pressure drops can be made since the flux of water has been shown to be a linear function of the pressure drop for both nanotubes (Corry, 2008) and for graphene nanopores (Cohen-Tanugi and Grossman, 2012). The conductance of water and ions through (20,0) carbon nanotubes as a function of simulation time is shown in FIGS. 9A and 9B, respectively. Conductance of water and ions per carbon nanotube (20,0) for pristine (non-functionalized) nanotubes (black line with solid square), carbon nanotubes with one zwitterion (1 ZI) at each end (blue line with empty triangle), and with two zwitterions (2 ZI) at each end (red line with solid circle) for a bulk concentration of 0.6 M NaCl and a pressure drop of 208 MPa is shown. Error bars show the standard deviation based on four independent simulations. The

linear increase in conductance with time indicates that the simulations are at steady state. FIGS. 9A and 9B demonstrate that as the number of zwitterion functional groups per tube increases, the conductance of both water and ions decreases. When each tube end was functionalized with two zwitterions, the conductance of ions decreased to zero while the flow rate of water was reduced, although its magnitude was still significant—about 100 water molecules per tube per ns. The calculated ion rejection ratio was 100% for the system with two zwitterions per tube; no ions passed through the carbon nanotubes over a total simulation time of 8 ns. The (20,0) carbon nanotubes with a single zwitterion on each end has an ion rejection ratio of about 25% and a water flow rate of about 450 H_2O molecules per nanotube per ns. According to embodiments of the invention nanotubes, for example, carbon nanotubes can be configured in a manner to provide for the flow of water through the nanotubes at a rate ranging for example between 0 and 2,000 water molecules per nanotube per ns, such as from about 50 to 1,000 water molecules per nanotube per ns, such as from about 150 to 750 water molecules per nanotube per ns, or from about 200 to about 600 water molecules per nanotube per ns, such as from about 300 to 500 water molecules per nanotube per ns, and so on. Alternatively or in addition, according to embodiments of the invention the nanotubes, such as carbon nanotubes, can be configured in a manner to provide for an ion rejection ratio of between 0 and 100%, such as from about 10-90%, or from 20-80%, or from 30-70%, or from about 40-60%, such as about 50%.

[00099] Also simulated were (20,0) carbon nanotubes with various numbers of carboxylic acid groups on each end. It was found that when five COOH groups are placed at each end that the water and ion flow rates are about the same as for the carbon nanotube with a single zwitterion on each end, with a water flow rate of 470 per tube per ns and an ion rejection ratio of about 20%. It is noted that the water flow rate is higher and the ion rejection ratio is lower for these simulations compared with those for a similar system reported by Corry (Corry, 2011). This is because a smaller diameter carbon nanotube was studied in that

work, namely the (8,8) carbon nanotube with a diameter of 1.1 nm. An ion rejection ratio of about 20% was measured. Simulations with 0.6 M KCl were carried out under the same conditions and have produced very similar results, as shown in FIGS. 16A and 16B. In particular, FIGS. 16A and 16B show conductance of (FIG. 16A) water and (FIG. 16B) ions per carbon nanotube for pristine (non-functionalized) nanotubes (black line with solid square), carbon nanotubes with one zwitterion (1 ZI) at each end (blue line with empty triangle), and with two zwitterions (2 ZI) at each end (red line with solid circle) for a bulk concentration of 0.6 M KCl and a pressure drop of 208 MPa. Error bars show the standard deviation based on four independent simulations.

[000100] The diameter distribution of carbon nanotubes used in experiments ranges from 10 to 20 Å, with an average diameter of 15 Å. NanoLab Inc. 179 Bear Hill Road, Waltham, MA 02451 ("NanoLab"). One or two zwitterion groups on one or both ends should be adequate to block all ion transport in carbon nanotubes having diameters less than 15 Å (*vide supra*). To demonstrate that ion transport can be blocked by the addition of zwitterions for the larger carbon nanotubes, a membrane composed of (26,0) carbon nanotubes was simulated, which have a diameter of 20.3 Å. Two, four, and five zwitterion groups were placed at the ends of each of the nanotubes in order to determine if zwitterions can completely block ion transport in these large diameter carbon nanotubes. As shown in FIGS. 10A and 10B, the conductance of water and ions for NaCl solutions was calculated at a pressure drop of 208 MPa through functionalized carbon nanotubes. Particularly, FIGS. 10A and 10B show conductance of (FIG. 10A) water and (FIG. 10B) ions per CNT (26,0) for CNTs with two zwitterions (2 ZI) at each end (black line with solid square), with four zwitterions at each end (blue line with empty triangle), and with five zwitterions (5 ZI) at each end (red line with solid circle) for a bulk concentration of 0.6 M NaCl at a pressure drop of 208 MPa. Error bars show the standard deviation based on four independent simulations. The concentration of saltwater is 0.6 M. The conductance of water and ions decreased as the number of zwitterion groups

was increased, as was the case with the (20,0) carbon nanotube membrane. When each tube end was functionalized with five zwitterion groups, the ion rejection ratio reached 100%; no ions passed through over a total simulation time of 8 ns. Thus, these simulations predict that even relatively large 20 Å diameter carbon nanotubes can have very high rejection ratios even when functionalized with a fairly small number of zwitterions.

[000101] Three polyamide membranes were fabricated with 0 (0 wt%), 0.25 mg (9 wt%) and 0.75 mg (20 wt%) of zwitterion-functionalized carbon nanotubes deposited in a plain polyamide matrix with total area of 17.35 cm^2. As a control, a fourth nanocomposite membrane containing 20 wt% end-capped carbon nanotubes was also fabricated. The area of each polyamide membrane that contained the carbon nanotubes was 10.75 cm^2 and was located in the center of the polyamide membrane. The weight percentage reflects the percentage of carbon nanotubes in the selective polyamide layer. These membranes were tested for water and ion flux by using a pressure drop of 3.65 MPa (530 psi) with a feed solution containing 1000 ppm (0.017 M) of NaCl.

[000102] The transport results are shown in FIG. 11. Particularly, FIG. 11 shows water flux (solid) and salt rejection ratio (hatched) as a function of CNT concentration in the selective PA layer of the nanocomposite membrane. The concentrations of zwitterion-functionalized CNTs (Z-CNTs) are 0 wt % (0mg), 9 wt% (0.25mg) and 20 wt% (0.75 mg) respectively. The concentration of end-capped CNTs (EC-CNTs) is 20 wt%. The concentration of NaCl is 1000 ppm. Pressure of 530 psi was applied for each membrane test. Error bars were computed from the standard deviations of the fluxes over a three day period. *See* FIGS. 17A-C. Adding 0.25 mg carbon nanotubes to the polyamide membrane resulted in the water flux increasing more than two-fold, from 6.8 GFD (gallons per square foot per day) to 14.0 GFD, while the rejection of Na^+ increased by approximately 1% from 97.6% to 98.5%. Increasing the amount of carbon nanotubes to 0.75 mg, the water flux increased by about a factor of four (to 28.5 GFD) over the plain polyamide membrane and the ion rejection ratio also

increased to 98.6%. FIG. 11 also shows that a significant increase in flux was achieved when 20 wt% closed-ended carbon nanotubes were incorporated into the polyamide matrix. However, this increase in water flux was accompanied by a drop in salt rejection down to 93%, which is lower than the salt rejection of the neat polyamide membrane.

[000103] Each membrane was tested for three consecutive days to examine the membrane stability. All membranes showed stable performance with < 1% variability over three days (*See* FIGS. 17A-C). It is noted that commercial polyamide membranes have significantly better performance than the tested membranes due to differences in the synthetic procedure. *See* Xie, W.; Geise, G. M.; Freeman, B. D.; S., L. H.; Byun, G.; Mcgrath, J. E., Polyamide interfacial composite membranes prepared from m-phenylene diamine, trimesoyl chloride and a new disulfonated diamine, J. Membr. Sci., 403-404, 152-161 (2012) ("Xie *et al.*, 2012"). Because there is no trade-off between selectivity and permeability, the experimental results suggest that the functionalized carbon nanotubes impart an additional transport mechanism to the membrane. It is believed that this mechanism consists of fast fluid flow through the functionalized carbon nanotubes, whose zwitterionic groups block the entry of ionic species into the carbon nanotube pores, thereby enhancing the salt rejection. These results are entirely consistent with the simulation results for the idealized carbon nanotube membranes. Increasing the concentration of carbon nanotubes provided more channels for the transport of water through the polyamide membrane, while ions were still blocked due to the zwitterionic groups attached at tube ends. The carbon nanotubes are entirely embedded within the polyamide membrane and are not completely aligned within the polyamide. This means that there is considerable room for improvement in the synthesis of the composite membrane. An ideal membrane would have carbon nanotubes perfectly aligned with the direction of fluid flow and would percolate completely through the membrane, so that no fluid would have to permeate through the polymer. The tested membranes provide a proof that functionalized carbon nanotubes can enhance

both water flux and salt rejection.

[000104] The fact that the water flux of the end-capped carbon nanotube composite membrane also increases significantly in comparison to the neat polyamide membrane suggests the formation of nano-scaled voids at the interface between the carbon nanotubes and the polymer matrix, at least for the pristine carbon nanotubes. These nanochannels allow water and salt ion molecules to travel through the membrane close to the external surface of the carbon nanotubes at faster rates than across the polyamide thin layer, leading to a higher water flux but lower selectivity for water/salt ion. It is possible that these nanochannels also exist in the case of the zwitterion-functionalized carbon nanotube composite membranes. Since the zwitterionic functional groups are attached not only at the pore entrance of the carbon nanotubes, but also along the wall of SWNTs, they can reject salt ions by size exclusion and Donnan exclusion at the entrance as well as inside the nanochannels. It is thus possible that water molecules travel both inside the SWNTs and around them in the nanochannels. For functionalized carbon nanotubes, both of the paths could be blocked by the zwitterionic groups, which offer good water/ions selectivity.

[000105] An alternate scenario is that the end-capped carbon nanotubes induce voids in the polyamide membrane while the zwitterion-functionalized carbon nanotubes do not. This is based on the following differences between the end-capped and zwitterion-functionalized carbon nanotubes: 1) The end-capped carbon nanotubes are about a factor of five longer than the zwitterion-functionalized tubes, the former being as long as 5 μm, while the latter are about 1 μm in length (NanoLab). It is reasonable to assume that these very long carbon nanotubes will disrupt the polyamide membrane structure to a much larger degree than the shorter carbon nanotubes. 2) The end-capped carbon nanotubes likely have pristine surfaces with very few functional groups covalently bound to them. In contrast, it is estimated that each zwitterion-functionalized carbon nanotube will have about 6.4×10^3 zwitterions or an average of about one zwitterion for every 30 carbon atoms on the carbon nanotube (see Appendix

below). This means that most of the zwitterions will be bound to and distributed along the sidewalls of the carbon nanotubes because the ends can only accommodate a small number of functional groups. For example, a (20,0) carbon nanotube could have a maximum of 20 zwitterions on each end. Hence, the interfacial surface energies of the end-capped and zwitterion-functionalized carbon nanotubes will be very different. It is reasonable to assume that the zwitterions will impart a greater degree of compatibility with the polyamide, hence, there may not be voids around the zwitterion-functionalized carbon nanotubes. This hypothesis is consistent with experiments showing that the pristine end-capped carbon nanotubes required the addition of surfactant to be dispersed in the polyamide, while the zwitterion-functionalized carbon nanotubes were dispersible in the absence of surfactant (see the Methods section below).

[000106] It is reasonable to assume that the reduction in water and ion flux in the functionalized nanotubes, shown in FIGS. 9A and 9B, is due to a combination of both the steric and electrostatic effects when adding additional zwitterions. In order to quantify the relative importance of electrostatic and steric effects, simulations were carried out with the partial charges of the zwitterion groups turned off—something that is impossible to do in an experiment. FIGS. 12A and 12B show conductance of (FIG. 12A) water and (FIG. 12B) ions through carbon nanotubes functionalized with one or two zwitterions per tube end and with charges on the zwitterions turned on or off. The diameter of each tube is 15.6 Å, corresponding to carbon nanotube (20,0). The pressure drop was 208 MPa in each case. Error bars show the standard deviation based on four independent simulations. As shown in FIGS. 12A-B, the conductance of both water and ions increased by about 30% in the 1 zwitterion system when the charges were turned off. In the 2 zwitterion system the ion rejection remained at 100% when the zwitterion charges were turned off, whereas the water conductance increased by about 35%, which is a modest increase given that the drop in water flux from unfunctionalized to functionalized with 2 zwitterions is about one order of magnitude. This indicates that steric hindrance is the dominant mechanism for

reducing the ion and water flux. The simulations for uncharged groups predict that hydrocarbon functional groups could block ion transport as well. However, the zwitterions impart compatibility with the polyamide polymer that may be missing in the hydrocarbon functional groups. Moreover, uncharged groups would not show any resistance to biofouling. A similar gating of carbon nanotubes was reported by Majumder based on experimental work on multi-walled nanotubes having much larger diameters that were functionalized with charged molecular tethers (Mujumder *et al.*, 2007).

[000107] The molecular simulations described in this specification probe the details of the steric hindrance due to the zwitterions. Unlike short functional groups, such as carboxylic acids, the zwitterions used in the experiments and simulations described herein are very flexible and can adopt a large number of different conformations. This flexibility is manifested in the simulations by noting that zwitterions, which are initially placed into the solution with their molecular chains in an extended (unfolded) configuration away from the tube pores, tend to fold during the course of the simulation so that they are at least partially folded inside the tube. The configuration of the zwitterion has a profound effect on the flux of water and ions. When the zwitterion is extended into the solution phase, transport of both ions and water occurs with much less resistance than when the zwitterions are folded into the tube. Steric effects dominate the transport of water and ions in this latter case. It is therefore very important to identify the free energy of the various configurations of the zwitterions. FIG. 13D shows the computed potential of mean force (PMF) for the change of free energy for a zwitterion functional group as it moves from a configuration where it is folded inside the nanotube (folded) and to a configuration where it is extended outside the nanotube into the solution phase (unfolded). A system composed of (20,0) carbon nanotubes functionalized with one or two zwitterions per nanotube end and a system composed of (26,0) carbon nanotubes functionalized with two or five zwitterions per tube end was studied. The PMF curves are in FIG. 13D.

[000108] FIG. 13A-C show configurations of zwitterions that are extended

(unfolded) into the liquid phase or folded inside the carbon nanotube for the (20,0) system with (FIG. 13A) one (1 ZI) or (FIG. 13B) two zwitterions (2 ZIs) per tube end and for the (26,0) system with (FIG. 13C) five zwitterions (5 ZIs) per tube end. FIG. 13D shows the PMF diagram of moving one zwitterion group from inside (folded) to outside (unfolded) of the carbon nanotube. FIG. 13D shows PMF for moving one zwitterion in a (20,0) carbon nanotube having one (red) or two (blue) zwitterions per tube end. FIG. 13E shows the PMF for moving one zwitterion in a (26,0) carbon nanotube having two (green) or five (black) zwitterions per tube end. The carbons on the carbon nanotube and zwitterion groups are shown as cyan. Oxygen, nitrogen and hydrogen are shown as red, purple and white. The terminal carbon on the zwitterion, shown in yellow in (A, B and C), was constrained in the umbrella sampling simulations. The tube end positions are represented as vertical dash lines in D.

[000109] It can be seen from FIGS. 13D-E that the free energy favors the folded configurations for all systems studied. The zwitterions tend to block tube entrances to reduce the effective pore size when they are folded inside the tubes, which is consistent with observations shown in FIGS. 12A and 12B that steric effects dominate over electrostatics. In the system with the (20,0) carbon nanotube (FIG. 13D), it is estimated that the folded configuration is about 2.9 kcal/mol more favorable than the unfolded configuration for a single zwitterion, and about 2.3 kcal/mol more favorable for having the second zwitterion folded inside the carbon nanotube when there are two zwitterions per tube end. The folded configuration is about 1.6 kcal/mol more favorable than the unfolded configuration for the (26,0) carbon nanotube system with two zwitterions (FIG. 13E).

[000110] When there are five zwitterions per tube end, the folded configuration is about 0.5 kcal/mol more favorable than the unfolded configuration, given that the other four zwitterions folded inside the carbon nanotube. The (20,0) and (26,0) carbon nanotubes have slightly different lengths in the simulations, as discussed in more detail below in the Methods section.

[000111] Salt Concentration Effects. The effect of salt concentration on the ion rejection ratio from both simulations and experiments was studied. The system with one zwitterion group per tube in simulations was studied because two zwitterions per tube end showed total rejection, dominated by steric effects (FIGS. 12A and 12B), and would therefore be less sensitive to changes in ion concentration. Flux simulations were carried out for 0.6 and 0.3M NaCl and KCl solutions (35000 and 17500 ppm for NaCl, 44700 and 22350 ppm for KCl), both with a pressure drop of 208 MPa. Simulations for 36 ns were run in order to gather accurate statistics for the ion rejection ratio as a function of concentration. The results are shown in the table of FIG. 14. Particularly, FIG. 14 shows water and ion flow rate (number per ns per carbon nanotube) and ion rejection ratio as a function of salt concentration for flow through a (20,0) carbon nanotube having one zwitterion functional group at each end. The simulations indicate that the salt concentration has no effect on the ion rejection ratio, at least for concentrations in the range 0.3 to 0.6 M. Simulations at much lower concentrations, as those used in experiments, were not feasible because of the low flux of ions and resulting poor statistics.

[000112] The concentration of NaCl in experiments was varied between 50 to 2000 ppm to test for ion concentration effects. Experiments were performed with both the plain polyamide membrane (no carbon nanotubes) and the nanocomposite membrane with 20 wt% carbon nanotubes in order to test for differences in concentration dependence inherent in the polyamide membrane as opposed to the functionalized carbon nanotubes. The results of these experiments are plotted in FIG. 15. In particular, FIG. 15 shows salt rejection as a function of NaCl feed concentration in plain PA (black curve with open circle) and a nanocomposite with 20 wt % carbon nanotubes (orange curve with solid circle). Feed pressure was 530 psi. The graph of FIG. 15 shows an increase in the salt rejection ratio with ion concentration for both the plain polyamide membrane and the nanocomposite membrane with 20 wt% carbon nanotubes.

[000113] The increase in rejection ratio with increasing ion concentration is

an unexpected result; indeed, the opposite effect was observed by Fornasiero *et al.*, who found that the ion rejection ratio decreased with increasing ion concentration in the feed, and dropped to zero when the ion concentration was equal to 10 mM (about 750 ppm) for KCl (Fornasiero et al, 2008). The difference in the performance between these prior membranes and membranes of the present invention is due to the mode of ion rejection. Fornasiero *et al.* used negatively-charged carbon nanotubes membranes, which rejected ions in accordance with the Donnan equilibrium theory (Fornasiero *et al.*, 2008). Many nanofiltration membranes are negatively charged and exhibit electrostatic screening effects. (*See* Bellona, C.; Drewes, J. E.; Xu, P.; Amy, G., Factors affecting the rejection of organic solutes during NF/RO treatment - a literature review, Water Research, 38, 2795-2809 (2004); *see* also Chung, C. V.; Buu, N. Q.; Chau, N. H., Influence of surface charge and solution pH on the performance characteristics of a nanofiltration membrane, Sci. Technol. Adv. Mater., 6, 246-250 (2005); and *see* Peeters, J. M. M.; Boom, J. P.; Mulder, M. H. V.; Strathmann, H., Retention measurements of nanofiltration membranes with electrolyte solutions, J. Membr. Sci., 145, 199-209 (1998).) Therefore, ion rejection is sensitive to salt concentrations in charged membranes. In contrast, Ji *et al.* showed that addition of zwitterionic groups counteracts the effects of ion concentration. *See* Ji, Y.-L.; An, Q.-F.; Zhao, Q.; Sun, W.-D.; Lee, K.-R.; Chen, H.-L.; Gao, C.-J., Novel composite nanofiltration membranes containing zwitterions with high permeate flux and improved anti-fouling performance, J. Membr. Sci. 390, 243-253 (2012) ("Ji *et al.*, 2012"). They demonstrated that the ion rejection ratio decreased from 95 to 60% as salt concentration was increased from 100 to 3500 ppm for a membrane without zwitterions. However, the addition of zwitterion groups to the membrane gave very stable rejection ratios that were independent of salt concentration (Ji *et al.*, 2012). Note that the plain polyamide membrane tested herein, which is uncharged, exhibits an increase in the rejection ratio with increasing concentration of NaCl (over a narrow range of concentrations). This same trend has been observed for other polyamide-type membranes. (*See* Yu, S.; Liu, M.; Lue, Z.; Zhou, Y.; Gao, C., Aromatic-

cycloaliphatic polyamide thin-film composite membrane with improved chlorine resistance prepared from m-phenylenediamine-4-methyl and cyclohexane-1,3,5-tricarbonyl chloride, J. Membr. Sci., 344, 155-164 (2009); *see* also Bandini, S.; Drei, J.; Vezzani, D., The role of pH and concentration on the ion rejection in polyamide nanofiltration membranes, J. Membr. Sci, 264, 65-74. (2005).) Therefore the increase in rejection ratio with increasing NaCl concentration observed for the nanocomposite membrane in FIG. 15 can be attributed to the polyamide component rather than the zwitterion-functionalized carbon nanotubes. This agrees with the molecular simulations described herein, showing no effect of concentration on the rejection ratio (FIG. 14).

[000114] This disclosure demonstrates that zwitterion-functionalized carbon nanotubes can be embedded in a polyamide membrane and that the performance of the composite membrane increases dramatically as the fraction of carbon nanotubes is increased. Both the water flux and ion rejection ratio increases, indicating that the increased water flux is not due to an increase in non-specific pores in the membrane, but rather due to an additional transport mechanism due to the presence of the functionalized carbon nanotubes. Molecular simulations show that the addition of only two zwitterions per nanotube end results in complete rejection of ions, while allowing significant water flux for nanotubes with diameters the same as those used in the experiments. This disclosure further demonstrates that the ion rejection occurs because of gaited entrance into the nanotubes due mainly to steric hindrance of the zwitterions, which adopt thermodynamically favored configurations so that they are folded into the tube end. Finally, the upper bound of membrane performance can be computed based on the simulation results for zwitterion-functionalized nanotube. Assuming a membrane containing 20 wt% carbon nanotubes, having lengths of 1000 nm, and assuming all carbon nanotubes are perfectly aligned (which is not the case in the experiments described herein), it is estimated that a flux of 20000 GFD will be exhibited for a membrane with a pressure drop of 530 psi (see Appendix below). This is three orders of magnitude greater than the

experimentally observed flow rate of 28.5 GFD, indicating that there is ample opportunity to optimize this first-generation membrane.

[000115] Materials and Methods.

[000116] Modeling. Molecular dynamics simulations were performed for hypothetical single-walled carbon nanotube membranes shown in FIG. 8. Two different membranes were considered, one composed of (20,0) carbon nanotubes and the other composed of (26,0) carbon nanotubes. The diameters of the carbon nanotubes were 15.6 and 20.3 Å, respectively. The length of the (20,0) carbon nanotubes was 41.18 Å, while the length of the (26,0) carbon nanotubes was 43.31 Å. The tubes had different lengths due to the inadvertent adding of a half of a unit cell to the (26,0) carbon nanotubes when constructing the tubes. This slight difference in length will not have any effect on the properties. The ends each tube were functionalized with 0, 1, or 2 zwitterionic groups for the (20,0) system and 2, 4, or 5 zwitterions for the (26,0) system. The carbon nanotubes were embedded in two graphene sheets to form a membrane. The membrane was immersed into a water box containing NaCl or KCl with periodic boundary conditions along three dimensions. The sizes of the simulation boxes were 54.1 Å × 55.38 Å × 114 Å for the (20,0) carbon nanotubes and 68.9 Å × 68.2 Å × 95.3 Å for the (26,0) system. The nominal concentration of salt in seawater of 0.6 M was used for most of the calculations. Selected calculations were also performed for a concentration of 0.3 M. The pressure of the bulk solution was equilibrated to 1 bar. Parameters for carbon atoms in carbon nanotubes and graphene sheets were taken as the parameters for aromatic carbon 'CA' in the CHARMM27 force field. (*See* Feller, S. E.; MacKerell, A. D., An improved empirical potential energy function for molecular simulations of phospholipids, J. Phys. Chem. B, 104, 7510-7515 (2000). ("Feller and MacKerell, 2000"); *see* also Klauda, J. B.; Brooks, B. R.; MacKerell, A. D.; Venable, R. M.; Pastor, R. W., An *ab initio* study on the torsional surface of alkanes and its effect on molecular simulations of alkanes and a DPPC bilayer, J. Phys. Chem. B, 109, 5300-5311 (2005) ("Klauda *et al.*, 2005")). All of the carbon atoms in carbon

nanotubes and graphene sheets were fixed in place during the dynamic simulation. It has been shown that the flexibility of carbon nanotubes only affects the kinetics of transport into a carbon nanotube when the pore entrance is about the same size as the molecule. *See* Bucior, B. J.; Chen, D.-L.; Liu, J.; Johnson, J. K., Porous Carbon Nanotube Membranes for Separation of H_2/CH_4 and CO_2/CH_4 Mixtures, The Journal of Physical Chemistry C, 116, 25904-25910 (2012). In the case of the present invention, the diameter of the carbon nanotubes is much larger than the size of the molecules and the gating effect is controlled by the zwitterion functional groups, which are fully flexible. Water molecules were simulated using the TIP3P water model. *See* Jorgensen, W. L.; Chandrasekhar, J.; Madura, J. D.; Impey, R. W.; Klein, M. L., Comparison of simple potential functions for simulating liquid water, J. Chem. Phys., 79, 926-935 (1983). The potential parameters for the zwitterion groups were also taken from the CHARMM27 force field (Feller and MacKerell, 2000; Klauda *et al.*, 2005) except for the atomic charges. The charges on the atoms of the zwitterions were obtained from an electrostatic potential fitting algorithm developed for periodic systems. *See* Chen, D. L.; Stern, A. C.; Space, B.; Johnson, J. K., Atomic Charges Derived from Electrostatic Potentials for Molecular and Periodic Systems, J. Phys. Chem. A, 114, 10225-10233 (2010) ("Chen *et al.*, 2010"). Details of the procedure are given in the Appendix below. The parameters for Na^+, K^+ and Cl^- were taken from the literature. (*See* Wander, M. C. F.; Shuford, K. L., Molecular Dynamics Study of Interfacial Confinement Effects of Aqueous NaCl Brines in Nanoporous Carbon, J. Phys. Chem. C, 114, 20539-20546 (2010). Dzubiella, J.; Hansen, J. P., Electric-field-controlled water and ion permeation of a hydrophobic nanopore, J. Chem. Phys., 122, 234706-14 (2005). The temperature of the system was controlled by a Nosé-Hoover thermostat with a damping parameter equal to 100. All calculations were performed with the LAMMPS package (*See* Plimpton, S., Fast parallel algorithms for short range molecular dynamics, J. Comp. Phys., 117, 1-19 (1995).) using a time step of 1fs. In the flux calculation, a pressure drop was introduced to generate the flux through the membrane using the method developed by Zhu *et al.* *See* Zhu, F. Q.;

Tajkhorshid, E.; Schulten, K., Pressure-induced water transport in membrane channels studied by molecular dynamics, Biophys. J., 83, 154-160. (2002). Following the approach of Corry (Corry, 2008; Corry, 2011) a constant force was applied to each water molecule in the force region of the saltwater box from 45 Å to 69 Å in the (20,0) system and from 40 Å to 55 Å in the (26,0) system.

[000117] Potential of mean force calculations for the zwitterion end group moving from inside to outside the nanotube were computed using the umbrella sampling method (*See* Torrie, G. M.; Valleau, J. P., Monte Carlo free energy estimates using non-Boltzmann sampling: Application to the sub-critical Lennard-Jones fluid, Chem. Phys. Lett., 28, 578-581 (1974).) in conjunction with weighted histogram analysis method (WHAM) using Grossfeld's code. *See* Grossfield, A. WHAM: the weighted histogram analysis method, 2.0.6; http://membrane.urmc.rochester.edu/content/wham: 2012 (2012). A one dimensional spring potential, $U=k_z(z-z_0)^2$, was applied along tube axis direction to each sampled zwitterion group. The spring force constant k_z was equal to 1 kcal/mol/Å^2. The sampling region from z=15.5 Å to z=35 Å was divided into 40 windows, the size of each window was equal to 0.5 Å. In the system with two zwitterions, another spring, $U'=k_z'(z-z_0')^2$, was applied to the unsampled zwitterion groups with z_0' =20.5 Å. This guaranteed that the second zwitterion group (unsampled zwitterion) remained around the tube end during the sampling for the first zwitterion group. The spring force constant k_z' was equal to 1 kcal/mol/Å^2. In the system with five zwitterion groups at each tube end, a larger spring force constant k_z= 3 kcal/mol/Å^2 was applied in order to improve sampling. The sampling time for each window was 500 ps with the first 100 ps discarded for equilibration. The convergence of the PMF calculations was checked by comparing PMF taking sampling times of 200, 300 or 400 ps for each window. Results from these shorter sampling times are in good quantitative agreement with the 500 ps sampling. Details of the WHAM method are given in the Appendix below.

[000118] Ion rejection ratio was calculated from simulations using:

$$R(\%) = (1 - \frac{J_{ion}}{J_{water}} \times \frac{C_{water}}{C_{ion}}) \times 100,$$

where J_{ion} and J_{water} are the conductance of ions and water, respectively, and C_{ion} and C_{water} are the concentrations of ions and water in the bulk phase, respectively. The concentrations of the bulk phase were taken to be constant and the flux was estimated by computing the ensemble average of the conductance of ions and water through the carbon nanotubes on a per-nanotube basis. Error bars were computed from the estimated sample standard deviations of the conductance, based on block averages.

[000119] Materials. The following chemicals were purchased from Sigma-Aldrich: 1,3,5- Benzenetricarbonyl trichloride (trimesoyl chloride, TMC), 1,3-phenylenediamine (m-phenylenediamine, MPD) and sodium dodecylbenzene-sulfonate (SDBS) were used as received. All chemicals were of analytical grade. Polyethersulfone (PES) ultrafiltration membranes were provided by Trisep Corp. (Goleta, CA).

[000120] Carbon Nanotube Functionalization. Carboxylate functionalized carbon nanotubes of outer diameter 15 Å and length 1μm were purchased from Nano Lab Inc. (Waltham, MA). (NanoLab). The COOH-functionalized carbon nanotubes were produced by chemical vapor deposition (CVD). Concentration of -COOH groups in the carbon nanotubes was approximately 2-7 wt% (as determined by titration). The functionalized carbon nanotubes were reacted with thionyl chloride ($SOCl_2$) at 65°C for 36 hours and the -COOH groups were replaced by COCl groups. The acylated carbon nanotubes were then esterificated using 3-dimethylamino-1-propanol, $(CH_3)_2$-N-C_3H_6-OH. This was followed by a ring-opening reaction of lactone, in which β-propiolactone was opened to form an acid group and attached to the tertiary amine on the functional group. (See Zhang, Z.; Chen, S.; Jiang, S., Dual-Functional Biomimetic Materials: Nonfouling Poly(carboxybetaine) with Active Functional Groups for Protein Immobilization. Biomacromolecules, 7, 3311-3315. (2006). Surapathi, A.; Chen, H.-y.; Marand, E.; Karl Johnson, J.; Sedlakova, Z., Gas sorption properties

of zwitterion-functionalized carbon nanotubes, Journal of Membrane Science, 429, 88-94 (2013). The resulting zwitterionic group had a positive charge at the tertiary amine group and negative charge at the carboxylated group.)

[000121] Membrane Fabrication. Functionalized carbon nanotube nano-composite membranes. Briefly, the fabrication process was divided into three steps, as shown schematically in FIGS. 3A-3C. First, the PES support was pretreated by soaking in 0.5 wt% SDBS solution to open the pores and to increase the hydrophilicity. Field emission scanning electron microscopy (FESEM) was used to examine the surface of the support, as shown in FIG. 18A and described in the Appendix below. The support was sandwiched between two round Poly(tetrafluoroethylene) (PTFE) holders. Afterwards, a predetermined amount of functionalized carbon nanotubes was poured on the support. High-vacuum filtration was used to disperse the carbon nanotubes on the support in a semi-aligned orientation (Kim *et al.*, 2007) and to remove the solvent. The third step in the membrane fabrication process was interfacial polymerization of polyamide. In this step, the support with semi-aligned carbon nanotubes was wetted in turn with 2 wt% MPD (with 0.2 wt% of SDBS) and 0.5% (w/v) TMC solutions before polymerization. The polyamide apparently completely covers the carbon nanotubes, as can be inferred by comparing the FESEM images for the plane polyamide and the carbon nanotube/polyamide membrane surfaces in FIGS. 18B and C. The partial alignment of the carbon nanotubes within the polyamide layer can be observed from the FESEM image of the cross section of the carbon nanotube/polyamide membrane shown in FIG. 18D. Details of the fabrication procedure are given in the Appendix below.

[000122] End-capped carbon nanotube nano-composite membranes. The end-capped SWNTs were purchased from NanoLab Inc. (NanoLab) and used as received without any further purification. They were produced by CVD method, with diameter of 15 Å and length of 1 to 5 μm. Unlike the zwitterionic functionalized SWNTs, end-capped SWNTs required the presence of surfactant in the solution to maintain a well-dispersed phase. In this case, 10 mg of SBDS

was added into 40ml of de-ionized water to create a 0.025 wt% SBDS solution. A certain amount of end-capped SWNTs, depending on the desired concentration of SWNTs in the membrane, was then dispersed in the SBDS solution by sonication. Using the identical fabrication method outline above, end-capped SWNTs were deposited and semi-aligned on a pretreated membrane support by filtration, followed with an interfacial polymerization of the polyamide carried out on the carbon nanotubes-attached support. After 5 min of oven curing, the fresh nanocomposite membrane was washed thoroughly with DI water, submersed in fresh DI water and stored in a laboratory refrigerator at 4 °C.

[000123] Membrane Characterization. Pressure-driven experiments were carried out on a laboratory-scale cross-flow membrane test unit, capable of pressures from 25 to 1000 psi. This test unit is comprised of a membrane cell (GE Sepa™ CF II Cell), high pressure pump (Hydra-cell pump, Warner Engineering), back-pressure regulator (US Paraplate), bypass valve (Swagelock), feed water reservoir (Nalgene), operated in closed loop mode with retentate being circulated into the feed water reservoir. The concentration analysis of the sodium cation present in the permeant was measured by a sodium ion-selective electrode (Thermo Scientific; 8611BNWP, MA).

[000124] Membrane Permeation tests. The membrane cell was pressurized to the designated hydraulic pressure by adjusting the speed of the pump and the flow rate of the retentate. For each testing pressure the permeation flux was allowed to equilibrate for 30 min before any permeant collection. A known amount of permeant was collected in a glass vial within a given period of time. The density of water was taken to be 0.997 g/cm^2 at ambient temperature, the volumetric flow rate was calculated from $Q = \frac{\Delta V}{tA}$, where ΔV is the permeate volume (US gallon), t is the permeation time (day) and A is the effective membrane area (ft^2). The flow rate, Q , is in the unit of gallon per square foot per day (GFD).

[000125] The sodium ion electrode was calibrated using a standard sodium solution with concentration of 1000 ± 5 ppm Na^+. The atomic absorption

spectrophotometer (AAS) was also calibrated using standard solutions, which contained 5, 10, 15 and 20 ppm of the specific cations, respectively. Thus, the concentrations of cations in the feed, C_f , and the permeant, C_p , were measured and the salt rejection ratio (in percent) was calculated from:

$$R(\%) = (1 - \frac{C_p}{C_f}) \times 100.$$

[000126] APPENDIX

[000127] Membrane Fabrication. The interfacial polymerization (IP) of polyamide is very sensitive to the operating condition and reaction time. Moreover, there are many ways to carry out the procedure. Different publications report different recipes in terms of the concentration of monomers, contact time, air-drying time, curing temperature, etc. *See* Ghosh, A. K.; Hoek, E.M.V., Impacts of support membrane structure and chemistry on polyamide-polysulfone interfacial composite membranes, J. Membr. Sci., 336, 140-148 (2009). Saha, N. K.; Joshi, S. V., Performance evaluation of thin film composite polyamide nanofiltration membrane with variation in monomer type. J. Membr. Sci., 342, 60-69. (2009). Kong, C.; Kanezashi, M.; Yamomoto, T.; Shintani, T.; Tsuru, T., Controlled synthesis of high performance polyamide membrane with thin dense layer for water desalination, J. Membr. Sci., 362, 76-80. (2010). (Xie *et al.*, 2012). A schematic of a recommended fabrication procedure is shown in FIGS. 3A-3C. The polyethersulfone (PES) membrane support was first pretreated by soaking in a 0.5 wt% sodium dodecylbenzenesulfonate (SDBS) solution (FIG. 3A) for two days to increase the hydrophilicity and to open the pores of the support. The support was then soaked in deionized (DI) water for one day to remove any excess surfactants. This soaking pretreatment guaranteed that there was no SBDS solution left in the pores. The absence of this step may introduce air bubbles underneath the later polyamide layer. The support was then sandwiched in between two round Poly(tetrafluoroethylene) (PTFE) holders. Before being poured on the top of the membrane support, a predetermined weight of zwitterion-functionalized carbon

nanotubes was dispersed in 40 ml of deionized (DI) water by sonication. During the sonication step, the carbon nanotube solution was heated by the sonicator horn and therefore required cooling to room temperature. As shown in FIG. 3B, the functionalized carbon nanotubes were deposited and semi-aligned on the membrane support using high-vacuum filtration (Kim, Jinschek, Chen, Sholl, and Marland, 2007) The support and carbon nanotubes were then dried for an hour in a vacuum oven. This insured that all water was removed from the nanotubes before the interfacial polymerization took place. An alternative way to filter the carbon nanotube solution was to use a solvent-resistant stirred cell (XFUF04701; Millipore, MA). This apparatus utilized a dead-end filtration method, in which the support was held at the bottom of the cell and the carbon nanotubes solution was stored within the cell above the support. The cell was pressurized up to 6 bar with inert gas on the top of the solution. Under this relatively high pressure the carbon nanotube solution also filtered through the support leaving the carbon nanotube behind. As shown in FIG. 3C, intrafacial polymerization was subsequently carried out on the carbon nanotube covered support by wetting the fabrication side (with carbon nanotubes) with an aqueous diamine solution containing 2 wt% MPD and 0.2 wt% of SDBS at ambient temperature for 2 min and then the membrane was unclamped and immediately placed on a glass plate. A glass roller was rolled over the membrane once to remove all the excess MPD solution. The membrane was then sandwiched again into the holder and wetted by a n-hexane solution containing 0.5% (w/v) TMC for 90 seconds. The resulting polyamide thin film nanocomposite membrane was subsequently heat cured at 68°C for 5 min. After the membrane had cooled down, it was washed thoroughly with DI water, submersed in fresh DI water and stored in a laboratory refrigerator at 4°C. The thickness and diameter of the interfacial polyamide layer (FIG. 3D) was approximately 500 nm and 3.7 cm, respectively. (*See* Zhao, J.; Wang, Z.; Wang, J.; Wang, S., Influence of heat-treatment on CO2 separation performance of novel fixed carrier composite membranes prepared by interfacial polymerization, J. Membr. Sci., 283, 346-356 (2006). Ghosh, A.K.; Jeong, B.-H.; Huang, X.;

Hoek, E.M.V., Impacts of reaction and curing conditions on polyamide composite reverse osmosis membrane properties, J. Membr. Sci., 311, 34-45 (2008).)

[000128] Carbon Nanotube Characterization. The surfaces and cross-section of the membranes were characterized by field emission scanning electron microscopy (FESEM, LEO 1550). Membrane samples were prepared for SEM cross-section imaging by gently peeling away the polyester backing fabric to ensure PES and zwitterion (Z)-carbon nanotubes/polyamide layers remained together. A small piece of fabric-free membrane sample was frozen in liquid nitrogen and fractured cryogenically. The surface morphologies of the PES support, polyamide and Z-carbon nanotubes/polyamide nanocomposite membranes were studied using FESEM and images are shown in FIGS. 18A-C, respectively. The cross-sectional view of the Z-carbon nanotubes/polyamide membrane, also taken by FESEM, is shown in FIG. 18D. The neat PES support (FIG. 18A) has a relatively smooth and porous surface with pore sizes ranging approximately from 6 to 20 nm. After interfacial polymerization, a thin polyamide skin layer with ridge- valley shape was formed on the top of the PES substrate (FIG. 18B) and acted as a barrier layer in separating salt ions from water. For the Z-carbon nanotubes/polyamide nanocomposite membrane (FIG. 18C), it can be seen that all the nanotubes were covered by interfacially polymerized polyamide. Due to the random packing of Z-carbon nanotubes, the surface roughness of the nanocomposite membrane is greatly increased relative to plain polyamide. The cross-section of the Z-carbon nanotubes/polyamide membrane (FIG. 18D) shows that nanotubes are embedded in polyamide with semi-aligned orientation (examples indicated by arrows).

[000129] Zwitterion Charge Fitting. Atom-centered charges for the zwitterions were obtained by computing the electrostatic potential of a zwitterion attached to the end of a (20, 0) carbon nanotube within density functional theory. The Perdew-Burke-Ernzenhof generalized gradient approximation functional as implemented within the Vienna Ab Initio Simulation Package was

used. (*See* Kresse, G.; Furthmüller, J., efficient iterative scheme for ab initio total energy calculations using a plane wave basis set, Phys. Rev. B, 54, 11169-11186 (1996); *see* also Kresse, G.; Furthmüller, J., Efficiency of ab initio total energy calculations for metals and semiconductors using a plane wave basis set, Comput. Mater. Sci. , 6, 15-50 (1996); *see* also Kresse, G.; Hafner, J., ab initio molecular dynamics simulations of the liquid metal amorphous semiconductor transition in germanium, Phys. Rev. B, 49, 14251-14269 (1994); *see* also Kresse, G.; Hafner, J., ab initio molecular dynamics for liquid metals. Phys. Rev. B, 47, 558-561 (1993).) An energy cutoff of 520 eV was used in the calculations. The resulting electrostatic potential was then fitted to point charges using the method of Chen *et al.* (Chen *et al.*, 2010). The resulting charges where then normalized so that the overall charge on the zwitterion was zero. This was needed because there were atom-centered charges on the carbon atoms of the nanotube, in addition to the zwitterion. However, the charges on the nanotube atoms were small in magnitude, so that the renormalization of the zwitterion charges made only minor changes to the computed values.

[000130] Estimation of Flow Rate Error Bars. The standard deviations for the flow rate calculations, shown in FIG. 14, were computed using block averages of the simulation data. The linear least squares method was used to fit a line to each block of data to get the flow rate (molecules/carbon nanotube/ns) in each block. $J_{water} - \sigma_{water}$. The standard deviation was calculated from:

$$\sigma = \sqrt{\frac{(J - \bar{J})^2}{n-1}},$$

where J is the flux of ions or water, and n represents the number of blocks. The errors in the ion rejection ratios were calculated by:

$$1-\frac{J_{ion}+\sigma_{ion}}{J_{water}-\sigma_{water}} \times \frac{C_{water}}{C_{ion}} < R < 1-\frac{J_{ion}-\sigma_{ion}}{J_{water}+\sigma_{water}} \times \frac{C_{water}}{C_{ion}}$$

where σ_{ion} and σ_{water} represent the standard deviations of the conductance of

ions and water.

[000131] Estimation of Flux Through an Ideal Membrane. In an ideal membrane all water flux will be through the carbon nanotubes and no water or ions would permeate through the polymer matrix. All the nanotubes would be semi-aligned so that they provided a pathway from one side of the membrane to the other. Taking the experimental membrane having 20 wt% (0.75 mg) carbon nanotubes, and assuming a nominal (20,0) carbon nanotube as the average nanotube having a length of 1000 nm, the average number of carbon nanotubes per membrane can be computed. The diameter of the membrane is 3.7 cm, so that the total area is 10.75 cm^2. This membrane would have a density of 1.86×10^{13} carbon nanotube/cm^2. Assuming a linear flux of water with pressure drop (Corry, 2008) a flux of 1.75 water molecules per carbon nanotube per ns can be obtained. Converting to units of gallons per square foot per day gives a flux of about 20,000 GFD at a pressure drop of 530 psi.

[000132] Estimation the Number of Zwitterions per Carbon Nanotube. In the experiment, the average diameter of carbon nanotubes is about 15 Å, close to the diameter of a carbon nanotube (20,0) which is 15.66 Å. Thus, the (20,0) carbon nanotube can be considered in the estimation of the number of zwitterions per carbon nanotube. In a carbon nanotube with indices 3π dcnt (n,m), the length of one unit cell is calculated as:

$$L = \frac{\sqrt{3}\pi d_{cnt}}{d_R}$$

(*See* Alexiadis, A.; Kassinos, S., Molecular Simulation of Water in Carbon Nanotubes, Chem. Rev., 108, 5014-5034 (2008) ("Alexiadis *et al.*, 2008")) where d_R is the common divisor for ($2n+m$, $2m+n$) and d_{cnt} is the diameter of a carbon nanotube. For a (20,0) carbon nanotube, L is given as 4.26 Å. The number of atoms in one unit cell of a carbon nanotube is calculated as:

$$n_c = \frac{4(n^2+m^2+nxm)}{d_R}$$

(Alexiadis *et al.*, 2008). Thus, in a (20,0) carbon nanotube, the number of atoms per unit cell is 80. The length of the carbon nanotubes used in experiments is around 1000 nm, so that the number of C atoms in one carbon nanotube is $\frac{80}{0.426nm}$ x 1000nm = $1.88x10^5$ atoms/carbon nanotube. The atomic percentages of C and N in zwitterion functionalized carbon nanotubes were measured by x-ray photoelectron spectroscopy. The results show that for every 100 atoms of the sample, 77 are C atoms and 2 are N atoms. Zwitterion groups we used have the structure: $-COO-(CH_2)_3-N^+(CH_3)_2-(CH_2)_2COO-$. Thus, each zwitterion group has one nitrogen atom and hence there are 2 zwitterion groups per 77 carbon atoms. For 77 carbon atoms, 18 of them are carbon atoms contained in the zwitterion groups. Let the number of zwitterion groups in a typical carbon nanotube be x. Using proportionality, x is calculated as $\frac{77-18}{2}$ = 29.5 = $\frac{1.88x10^5}{x}$. Therefore, the number of zwitterions is estimated to be 6400 per carbon nanotube. Given that there are only 20 dangling bonds at each end of a (20,0) carbon nanotube, the maximum number of zwitterions attached at the ends is 40. Thus, most of zwitterions must be bound to the tube wall, presumably at defect sites along the length of the nanotube.

[000133] Weighted Histogram Analysis. The initial configuration for each window before the sampling is an equilibrated state. In order to reach that equilibrated configuration, two simulation steps before sampling were performed. Firstly, starting from one configuration with the sampled carbon atom located in the interior of the pore, the sampled carbon atom was moved to the center of the target window by applying a one dimensional spring $U=k_z(z-z_0)^2$ with force constant of k_z=50 kcal/mol/Å^2 to the sampled carbon atom for a short MD run of 100 ps. Secondly, the system was equilibrated with the same spring potential for 500 ps to ensure that the sampled atom was located near the center of the window. Next, the sampling was started by using a one dimensional spring with a force constant of 1 kcal/mol/Å^2. The sampling process lasted for

500 ps. The initial 100 ps was discarded and only the last 400 ps was used for the WHAM analysis.

[000134] The present invention has been described with reference to particular embodiments having various features. It will be apparent to those skilled in the art that various modifications and variations can be made in the practice of the present invention without departing from the scope or spirit of the invention. One skilled in the art will recognize that other variations may be substituted for those described herein that fall within the scope and spirit of the invention. Other embodiments of the invention will be apparent to those skilled in the art from consideration of the specification and practice of the invention. The description of the invention provided is merely exemplary in nature and, thus, variations that do not depart from the essence of the invention are intended to be within the scope of the invention. In methods according to the invention, e.g., one, all, or some of the method steps can be used and where feasible in any order or in any combination. It is further noted that each of the references cited in this specification is hereby incorporated by reference herein each in its entirety.

CLAIMS

1. A method of fabricating functionalized carbon nanotube nanocomposite membranes, comprising:

functionalizing one or more carbon nanotube with one or more zwitterionic functional group to provide one or more functionalized carbon nanotubes;

depositing the one or more functionalized carbon nanotubes on a support;

depositing a polymer on the support to provide a polymer matrix comprising the polymer and the functionalized carbon nanotubes, thereby forming a nanocomposite membrane;

wherein the one or more zwitterionic functional groups comprise less than 18 carbon atoms and the polymer is one or more of polyamide, polyurea, polyimide, polycarbonate, polymethacrylate, polysulphone, or other thermoplastic polymer, cellulose acetate (CA), cellulose triacetate (CTA), or other cellulosic polymer.

2. The method of claim 1, wherein the carbon nanotubes are single-walled, multi-walled, or double-walled carbon nanotubes.

3. The method of claim 1 or 2, wherein the zwitterionic functional groups comprise less than 16 carbon atoms.

4. The method of claim 1 or 2, wherein the zwitterionic functional groups comprise less than 14 carbon atoms.

5. The method of claim 1 or 2, wherein the zwitterionic functional groups comprise less than 12 carbon atoms.

6. The method of claim 1 or 2, wherein the zwitterionic functional groups comprise less than 10 carbon atoms.

7. The method of claim 1 or 2, wherein the zwitterionic functional groups comprise less than 8 carbon atoms.

8. The method of claim 1 or 2, wherein the zwitterionic functional groups

comprise less than 6 carbon atoms.

9. The method of claim 1 or 2, wherein the zwitterionic functional groups have the structure -COO-$(CH_2)_3$-$N^+(CH_3)_2$-$(CH_2)_2COO^-$.

10. The method of claim 1 or 2, wherein the carbon nanotubes comprise from 1 to 10 zwitterions at each end.

11. The method of claim 1 or 2, wherein the carbon nanotubes comprise from 1 to 5 zwitterions at each end.

12. The method of claim 1 or 2, wherein the carbon nanotubes comprise 1 zwitterion at each end.

13. The method of claim 1 or 2, wherein the carbon nanotubes comprise 2 zwitterions at each end.

14. The method of claim 1 or 2, wherein the carbon nanotubes comprise 4 zwitterions at each end.

15. The method of claim 1 or 2, wherein the carbon nanotubes comprise 5 zwitterions at each end.

16. The method of claim 1 or 2, wherein the carbon nanotubes comprise from 1 zwitterion to 10 zwitterions at one end.

17. The method of claim 1 or 2, wherein the carbon nanotubes have a pore diameter ranging from about 0.1 nm to about 50 nm.

18. The method of claim 1 or 2, wherein the carbon nanotubes have a length ranging from about 0.1 μm to about 10 μm.

19. The method of claim 1 or 2, wherein the carbon nanotubes are synthesized through one of arc discharge, laser ablation, plasma torch, high pressure CO disproportion, and chemical vapor deposition.

20. The method of claim 1 or 2, wherein the carbon nanotubes represent about 0.1% by weight to about 90% by weight of the polymer matrix.

21. The method of claim 1 or 2, wherein the carbon nanotubes represent

about 9% by weight of the polymer matrix.

22. The method of claim 1 or 2, wherein the carbon nanotubes represent about 20% by weight of the polymer matrix.

23. The method of claim 1 or 2, wherein functionalizing one or more carbon nanotube with one or more zwitterionic functional group comprises a reflux step, wherein carbon nanotubes are refluxed in sulfuric acid and nitric acid.

24. The method of claim 23, wherein functionalizing one or more carbon nanotube with one or more zwitterionic functional group comprises a thionyl chloride addition step.

25. The method of claim 24, wherein functionalizing one or more carbon nanotube with one or more zwitterionic functional group comprises a 3-(dimethylamino)propan-1-ol addition step.

26. The method of claim 25, wherein functionalizing one or more carbon nanotube with one or more zwitterionic functional group comprises a β-propiolactone addition step.

27. The method of claim 1 or 2, wherein depositing the one or more functionalized carbon nanotubes on a support comprises:

pretreatment of the support with a surfactant; and

filtration of a solution of the functionalized carbon nanotubes through the support.

28. The method of claim 27, wherein said surfactant is an anionic surfactant.

29. The method of claim 28, wherein said surfactant is sodium dodecyl benzene sulfonate.

30. The method of claim 27, wherein said filtration comprises high pressure filtration.

31. The method claim 27, wherein said filtration comprises vacuum filtration.

32. The method of claim 1 or 2, wherein depositing a polymer on the support

to provide a polymer matrix involves intrafacial polymerization.

33. The method of claim 32, wherein the support comprises a polyester side and a polysulfone side.

34. The method of claim 32, wherein intrafacial polymerization comprises:

contacting the polyester side of the support with an aqueous solution comprising a diamine;

removing said aqueous solution from the support; and

contacting the polysulfone side of the support with an organic solution comprising an acid chloride.

35. The method of claim 34, wherein said aqueous solution comprises m-phenylene diamine.

36. The method of claim 34, wherein the organic solution comprises trimesoyl chloride.

37. The method of claim 34, wherein the support comprises polyethersulfone (PES).

38. The method of claim 1 or 2, wherein the polymer is polyamide.

39. The method of claim 1 or 2, wherein the method is carried out on an industrialized scale for industrial membrane manufacture.

40. A method of carbon nanotube functionalization comprising:

a reflux step, wherein carbon nanotubes are refluxed in a combination of sulfuric acid and nitric acid;

a thionyl chloride addition step;

a 3-(dimethylamino)propan-1-ol addition step; and

a β-propiolactone addition step.

41. A method of deposition of carbon nanotubes on a membrane support comprising:

pretreatment of said membrane support with a surfactant; and

filtration of a solution of said carbon nanotubes through said membrane support.

42. The method of claim 41, wherein said filtration comprises high-pressure filtration.

43. The method of claim 41, wherein said filtration comprises vacuum filtration.

44. A method of intrafacial polymerization of polyamide on a membrane support, wherein the membrane support comprises a polyester side and polysulfone side, the method comprising:

contacting the polyester side of said membrane support with an aqueous solution comprising a diamine;

removing said aqueous solution from said membrane support; and

contacting the polysulfone side of said membrane support with an organic solution comprising an acid chloride.

45. The method of claim 44, wherein said aqueous solution comprises m-phenylene diamine.

46. The method of claim 44, wherein the organic solution comprises trimesoyl chloride.

47. The method of claim 44, wherein the membrane support comprises polyethersulfone (PES).

48. A method of intrafacial polymerization of polyamide on a membrane support, wherein the membrane support comprises a polyester side and polysulfone side, comprising:

contacting the polyester side of the membrane support with an organic solution comprising an acid chloride;

removing said organic solution from said membrane support; and

contacting the polysulfone side of said membrane support with an aqueous solution comprising a diamine.

49. The method of claim 48, wherein said aqueous solution comprises m-phenylene diamine.

50. The method of claim 48, wherein the organic solution comprises trimesoyl chloride.

51. The method of claim 48, wherein the membrane support comprises polyethersulfone (PES).

52. A functionalized carbon nanotube nanocomposite membrane fabricated according to the method of claim 1 or 2.

53. A functionalized carbon nanotube nanocomposite membrane, comprising:

a membrane support;

carbon nanotubes comprising zwitterionic functional groups disposed on said membrane support; and

a polymer disposed on said membrane support;

wherein the zwitterionic functional groups comprise less than 18 carbon atoms and wherein the polymer is one or more of polyamide, polyurea, polyimide, polycarbonate, polymethacrylate, polysulphone, or other thermoplastic polymer, cellulose acetate (CA), cellulose triacetate (CTA), or other cellulosic polymer.

54. The nanocomposite membrane of claim 53, wherein the carbon nanotubes are single-walled, multi-walled, or double-walled carbon nanotubes.

55. The nanocomposite membrane of claim 53 or 54, wherein the zwitterionic functional groups comprise less than 16 carbon atoms.

56. The nanocomposite membrane of claim 53 or 54, wherein the zwitterionic functional groups comprise less than 14 carbon atoms.

57. The nanocomposite membrane of claim 53 or 54, wherein the zwitterionic functional groups comprise less than 12 carbon atoms.

58. The nanocomposite membrane of claim 53 or 54, wherein the zwitterionic functional groups comprise less than 10 carbon atoms.

59. The nanocomposite membrane of claim 53 or 54, wherein the zwitterionic functional groups comprise less than 8 carbon atoms.

60. The nanocomposite membrane of claim 53 or 54, wherein the zwitterionic functional groups comprise less than 6 carbon atoms.

61. The nanocomposite membrane of claim 53 or 54, wherein the zwitterionic functional groups have the structure $-COO-(CH_2)_3-N^+(CH_3)_2-(CH_2)_2COO^-$.

62. The nanocomposite membrane of claim 53 or 54, wherein the carbon nanotubes comprise 1-10 zwitterions at each nanotube end.

63. The nanocomposite membrane of claim 53 or 54, wherein the carbon nanotubes comprise 1-5 zwitterions at each nanotube end.

64. The nanocomposite membrane of claim 53 or 54, wherein the carbon nanotubes comprise with 1 zwitterion at each nanotube end.

65. The nanocomposite membrane of claim 53 or 54, wherein the carbon nanotubes comprise 2 zwitterions at each nanotube end.

66. The nanocomposite membrane of claim 53 or 54, wherein the carbon nanotubes comprise 4 zwitterions at each nanotube end.

67. The nanocomposite membrane of claim 53 or 54, wherein the carbon nanotubes comprise 5 zwitterions at each nanotube end.

68. The nanocomposite membrane of claim 53 or 54, wherein the carbon nanotubes comprise 1-10 zwitterions at one nanotube end.

69. The nanocomposite membrane of claim 53 or 54, wherein the carbon nanotubes have a pore diameter ranging from about 0.1 nm to about 50 nm.

70. The nanocomposite membrane of claim 53 or 54, wherein the carbon nanotubes have a length ranging from about 0.1 μm to about 10 μm.

71. The nanocomposite membrane of claim 53 or 54, wherein the carbon

nanotubes are synthesized through one of arc discharge, laser ablation, plasma torch, high pressure CO disproportion, and chemical vapor deposition.

72. The nanocomposite membrane of claim 53 or 54, wherein the carbon nanotubes comprising zwitterionic functional groups and the polymer together comprise a polymer matrix and the carbon nanotubes are disposed in the polymer matrix in an amount ranging from about 0.1% by weight to about 90% by weight of the polymer matrix.

73. The nanocomposite membrane of claim 53 or 54, wherein the carbon nanotubes comprising zwitterionic functional groups represent about 9% by weight of a polymer matrix.

74. The nanocomposite membrane of claim 53 or 54, wherein the carbon nanotubes comprising zwitterionic functional groups represent about 20% by weight of a polymer matrix.

75. The nanocomposite membrane of claim 53 or 54, wherein the membrane support comprises polyethersulfone (PES).

76. The nanocomposite membrane of claim 53 or 54, wherein the membrane support comprises polyfluoroethylene (PTFE), polyvinylidene fluoride (PVDF), polypropylene, or nylon.

77. The nanocomposite membrane of claim 53 or 54, wherein the polymer comprises polyamide.

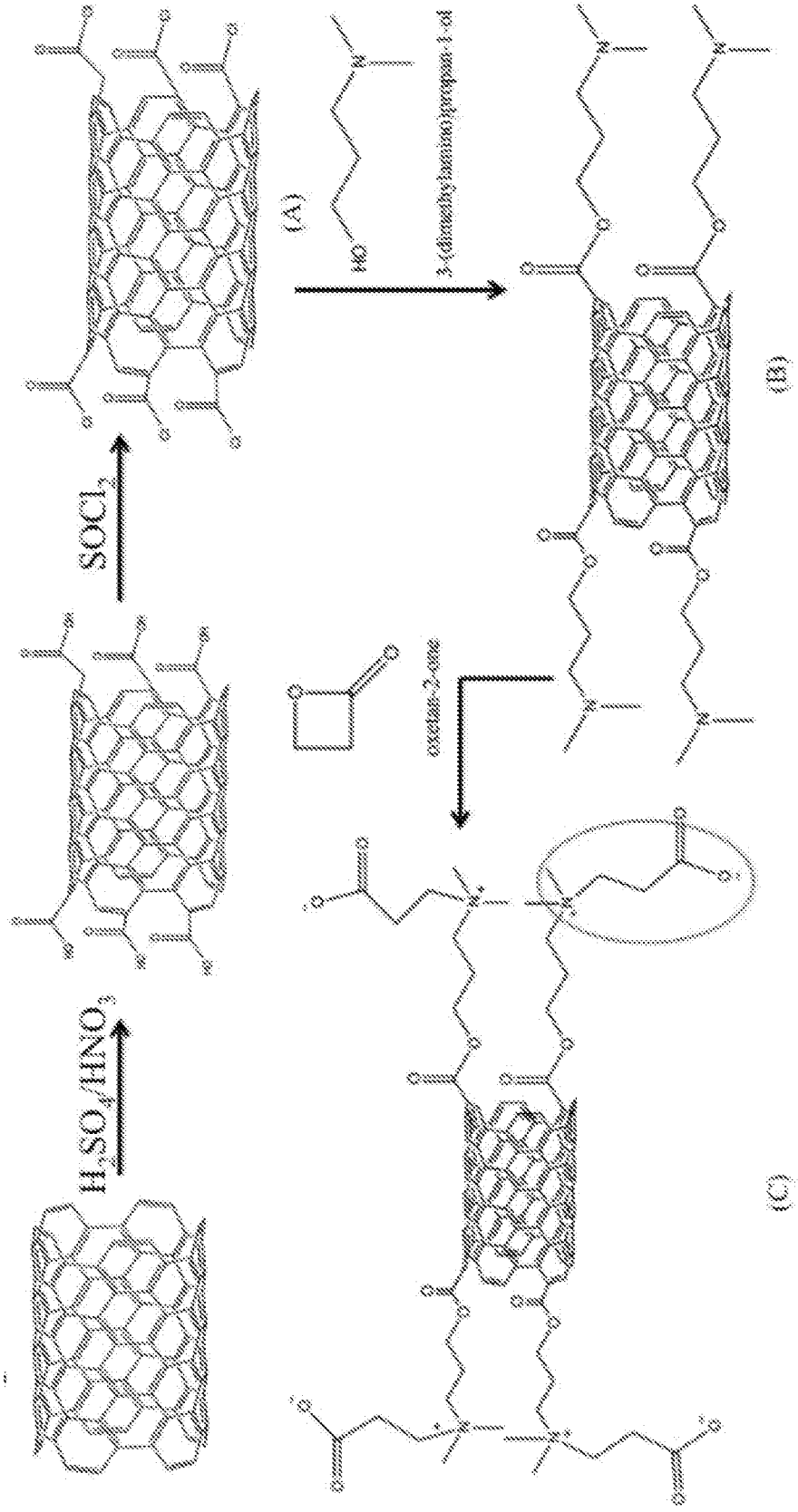
H_2SO_4/HNO_3
$SOCl_2$
(A)
HO
3-(dimethylamino)propan-1-ol
(B)
oxetan-2-one
(C)

FIG. 1

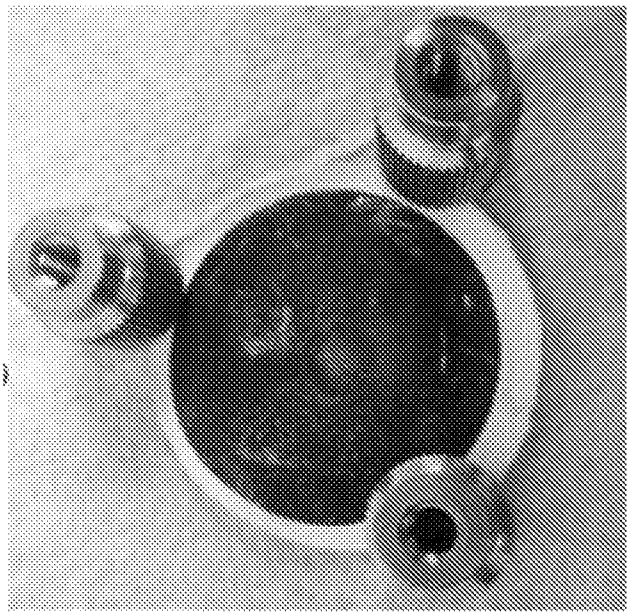

FIG. 2B

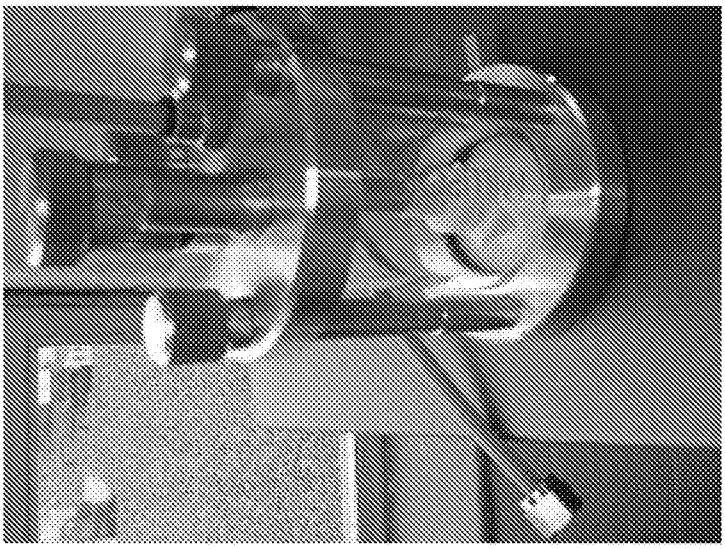

FIG. 2A

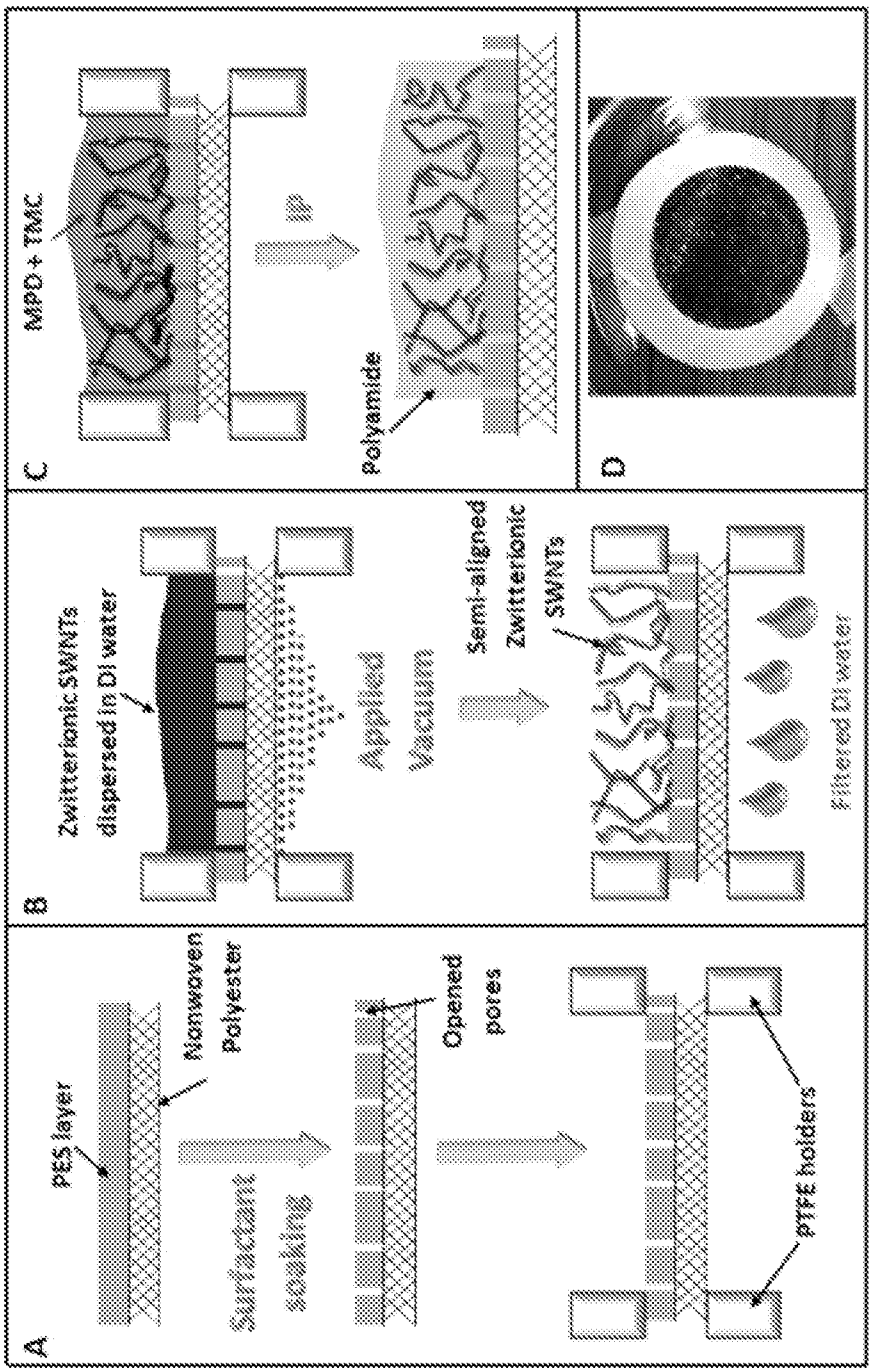
A
PES layer
Nonwoven Polyester
Surfactant soaking
Opened pores
PTFE holders
3A
B
Zwitterionic SWNTs dispersed in DI water
Applied Vacuum
Semi-aligned Zwitterionic SWNTs
Filtered DI water
3B
C
MPD + TMC
IP
Polyamide
3C
D
3D

FIGS. 3A-D

Functionalization of CNTs	Sample/Gas	H2	He	N2	O2	CH4	CO2	SF6
Zwitterion	PA (Z-CNT 0 mg)	325.1	249.96	155.65	76.65	203.4	70.85	65.35
	PA (Z-CNT 1 mg)	1912.03	1406.6	675.33	569.96	956.61	575.15	390.65
	PA (Z-CNT 1.5 mg)	2663.73	1803.7	766.79	775.95	1316.8	588.48	510.38
	PA (Z-CNT 2 mg)	2759.92	1963.37	956.76	804.76	1306.02	769.96	506.79
	PA (Z-CNT 5 mg)	8072.01	4862.7	2901.46	2506.1	4151	2613.79	1880.27
COOH	*PA (Z-CNT 1 mg)*	*3625.06*	*2479.44*	*1373.21*	*1020.86*	*1764.79*	*1166.79*	*827.13*

FIG. 4

	First Day		Second Day		Third Day	
430 Psi	-	-	11.86 GFD	98.22%	-	-
530 Psi	14.08 GFD	98.35%	13.30 GFD	98.70%	14.45 GFD	98.53%
620 Psi	12.73 GFD	98.50%	-		21.02 GFD	98.62%

FIG. 5A

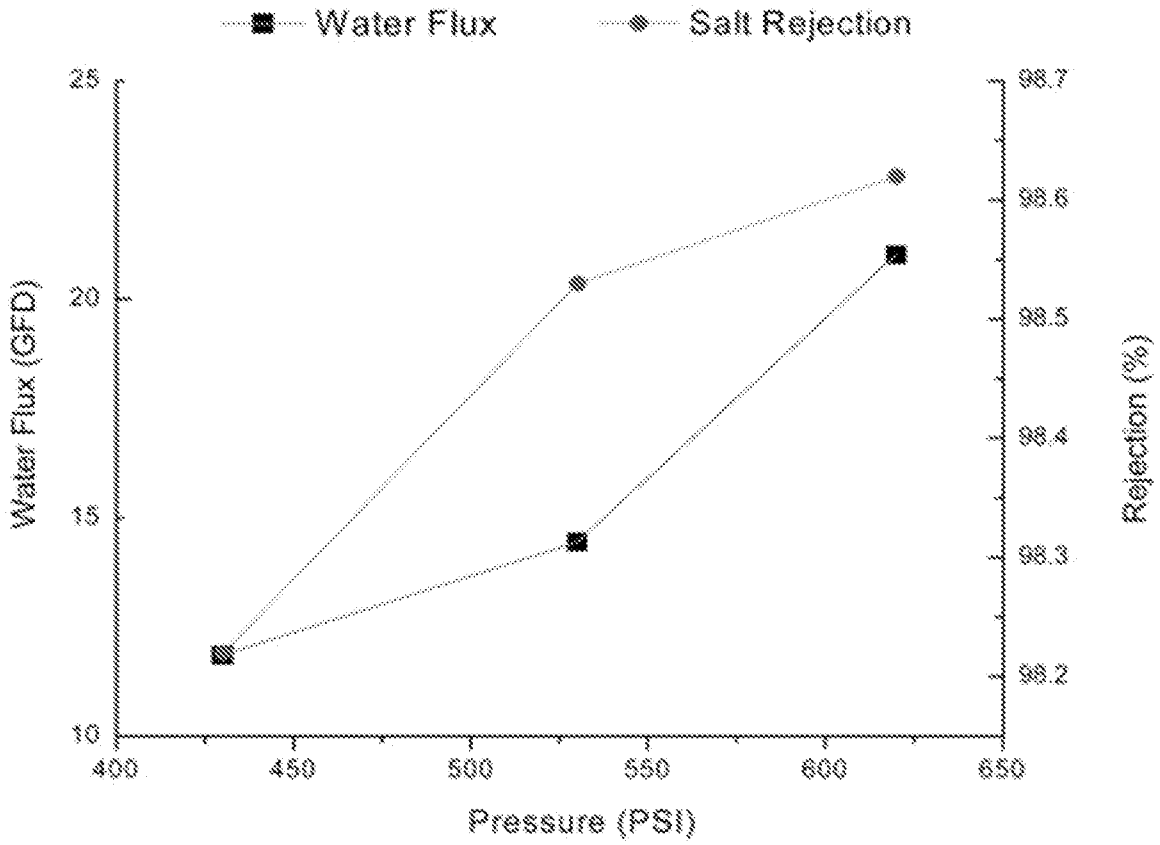

FIG. 5B

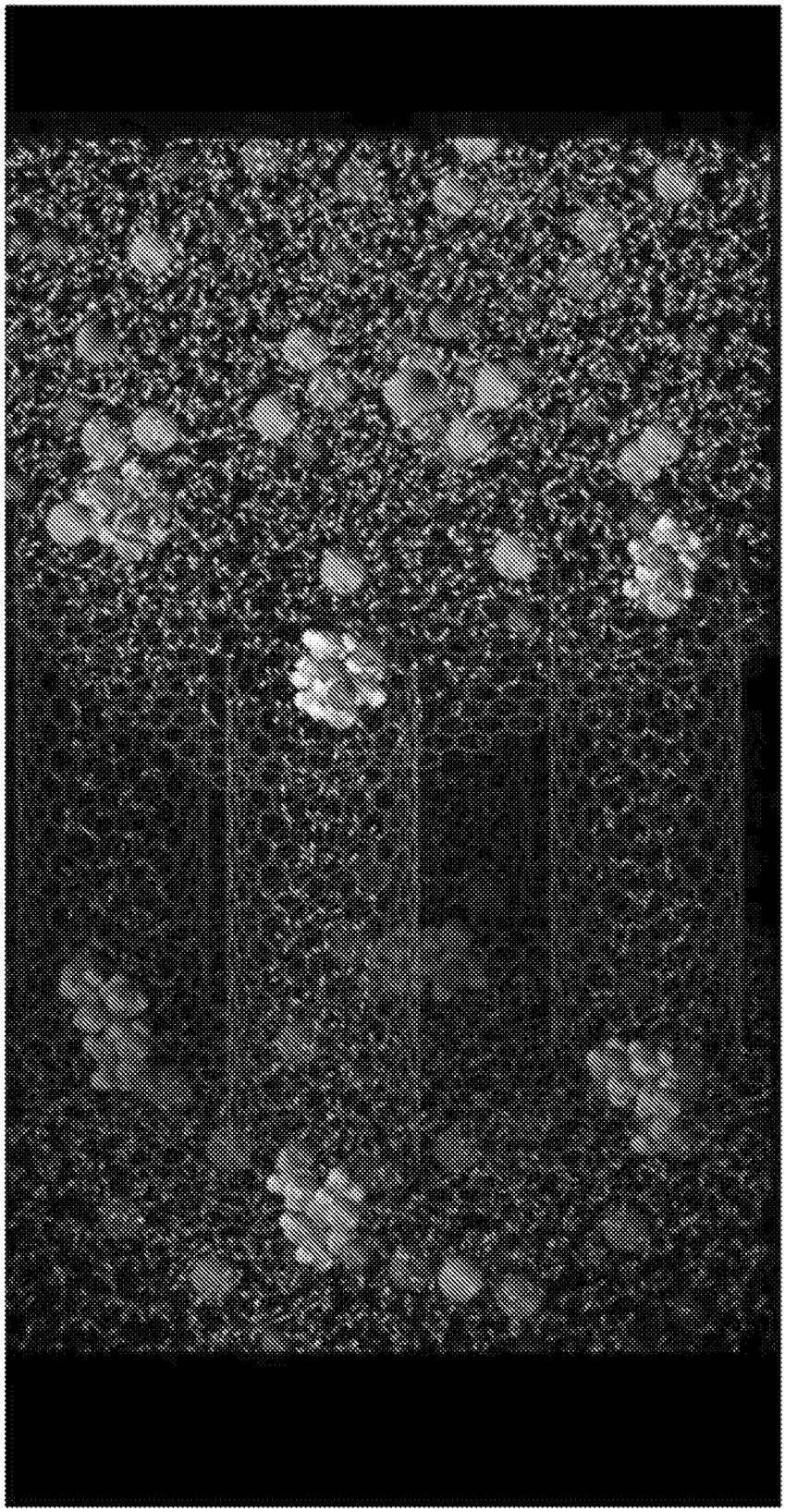

FIG. 6

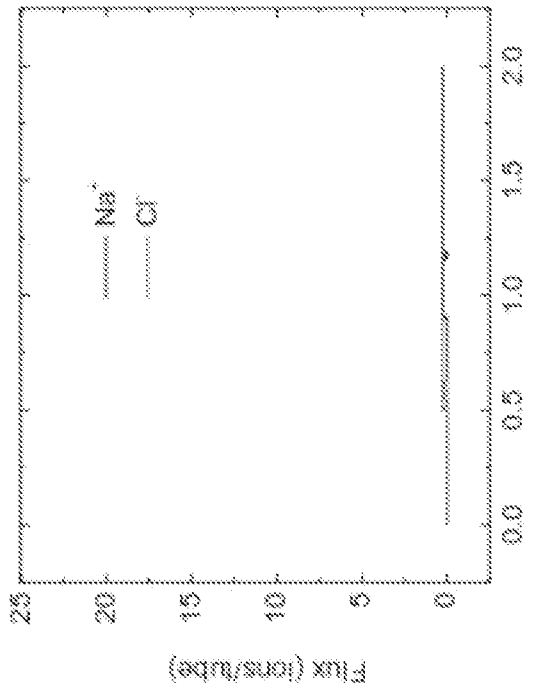
Flux (ions/tube)
25
20
15
10
5
0
0.0
0.5
1.0
1.5
2.0
Time(ns)
Na+
Cl-

FIG. 7B

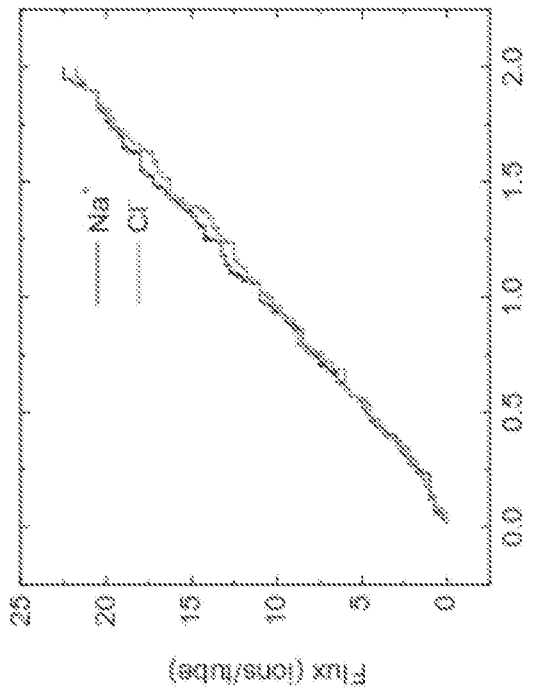
Flux (ions/tube)
25
20
15
10
5
0
0.0
0.5
1.0
1.5
2.0
Time(ns)
Na+
Cl-

FIG. 7A

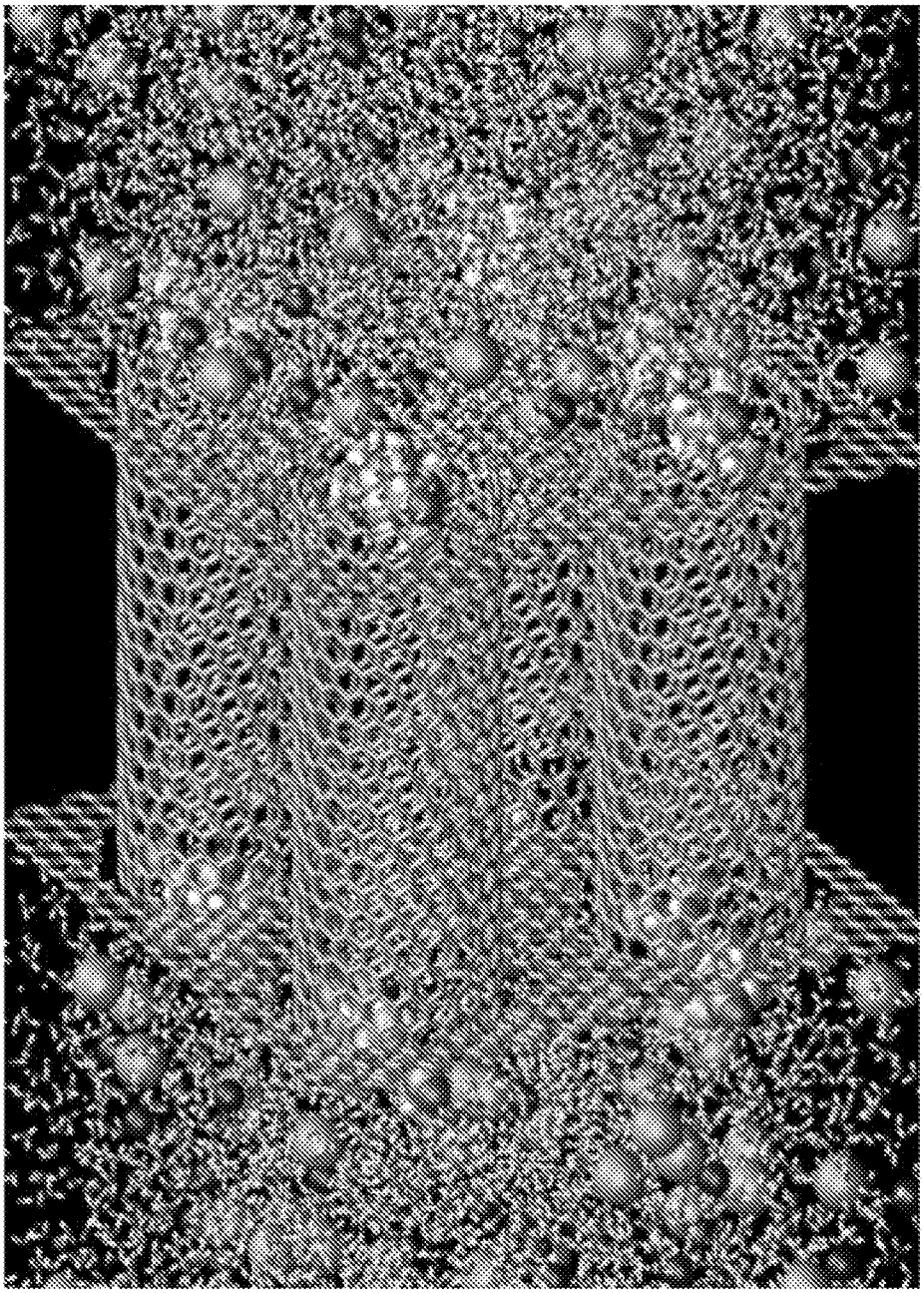

FIG. 8

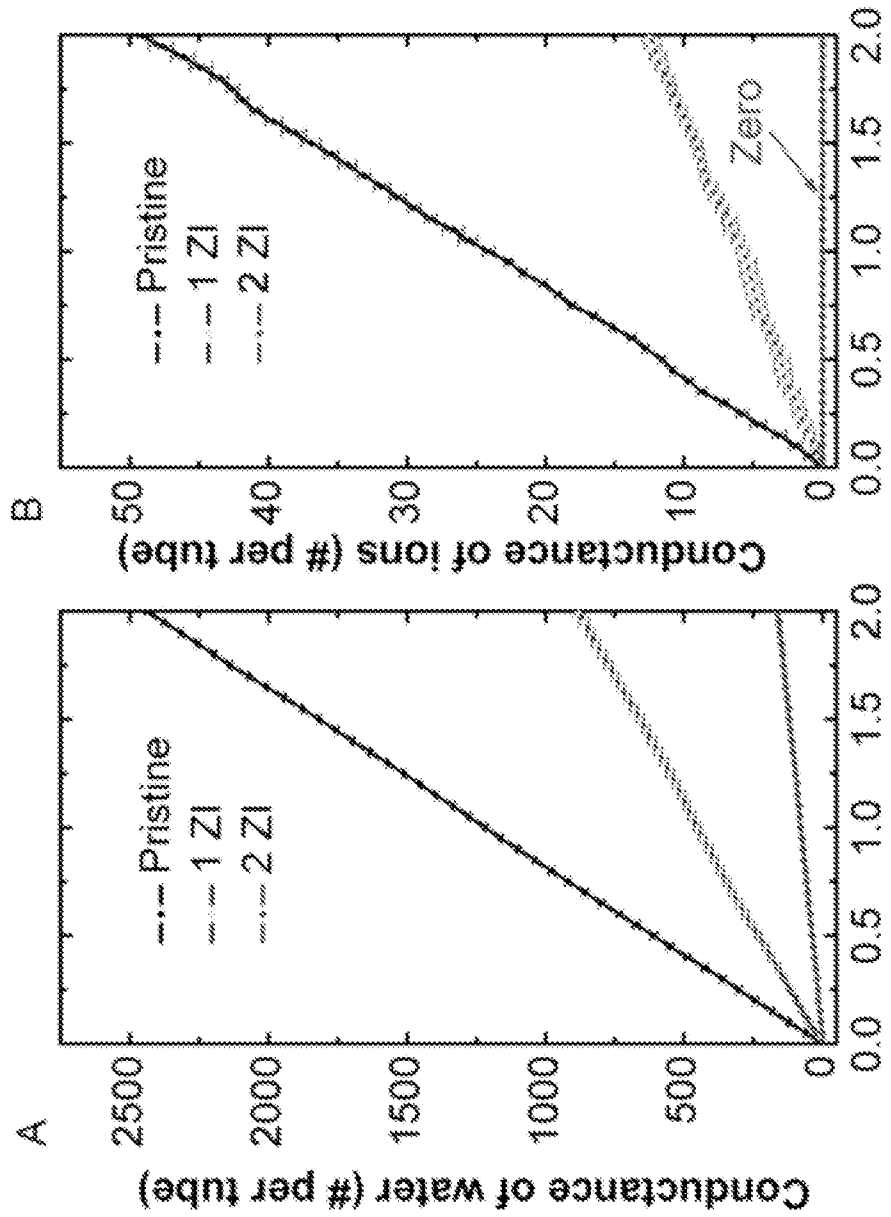
A
Conductance of water (# per tube)
2500
2000
1500
1000
500
0
Pristine
1 ZI
2 ZI
0.0
0.5
1.0
1.5
2.0
Time (ns)
B
Conductance of ions (# per tube)
50
40
30
20
10
0
Pristine
1 ZI
2 ZI
Zero
0.0
0.5
1.0
1.5
2.0
Time (ns)

FIG. 9A

FIG. 9B

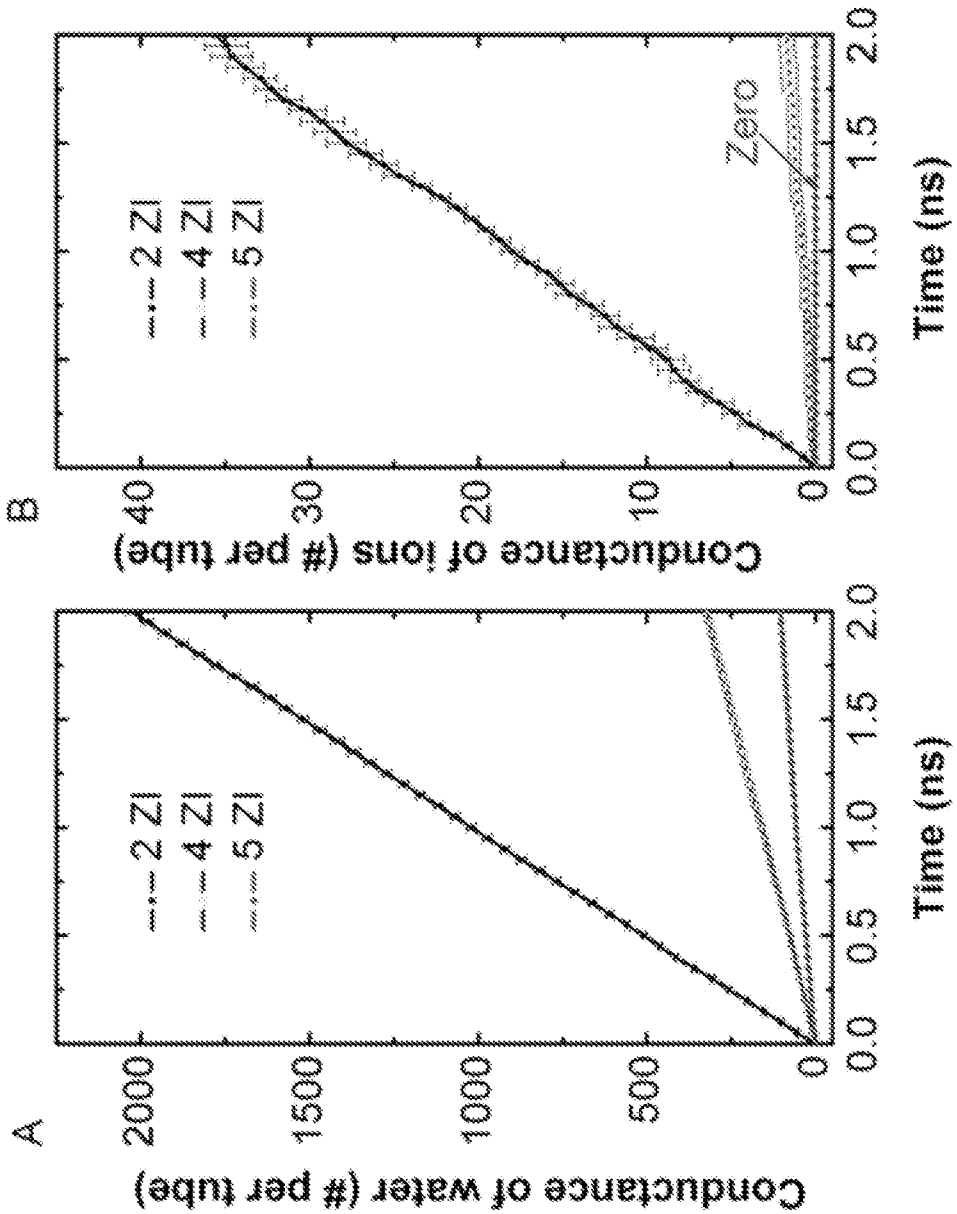

FIG. 10A

FIG. 10B

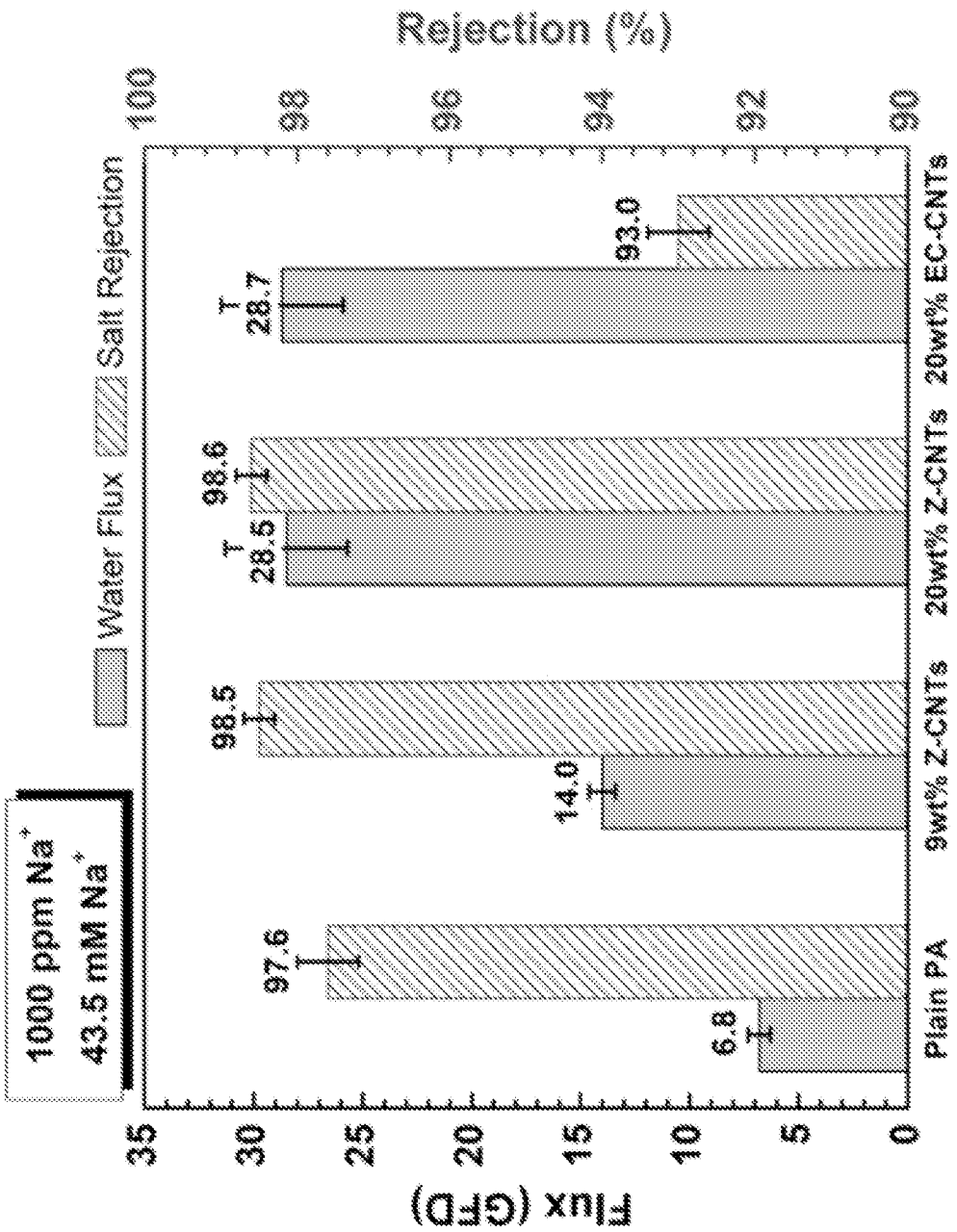
Rejection (%)
100
98
96
94
92
90
Water Flux
Salt Rejection
1000 ppm Na+
43.5 mM Na+
Flux (GFD)
35
30
25
20
15
10
5
0
97.6
6.8
98.5
14.0
98.6
28.5
93.0
28.7
Plain PA
9wt% Z-CNTs
20wt% Z-CNTs
20wt% EC-CNTs

FIG. 11

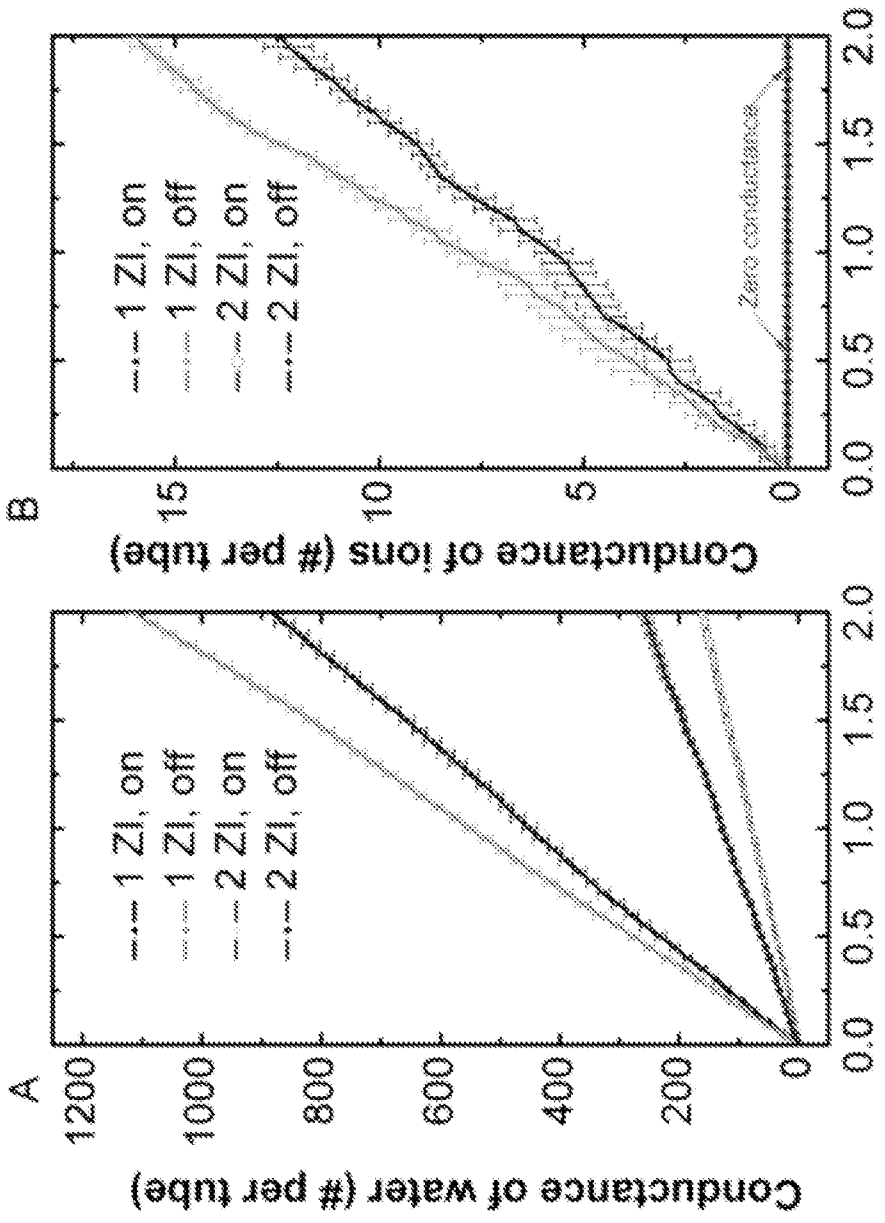

FIG. 12A

FIG. 12B

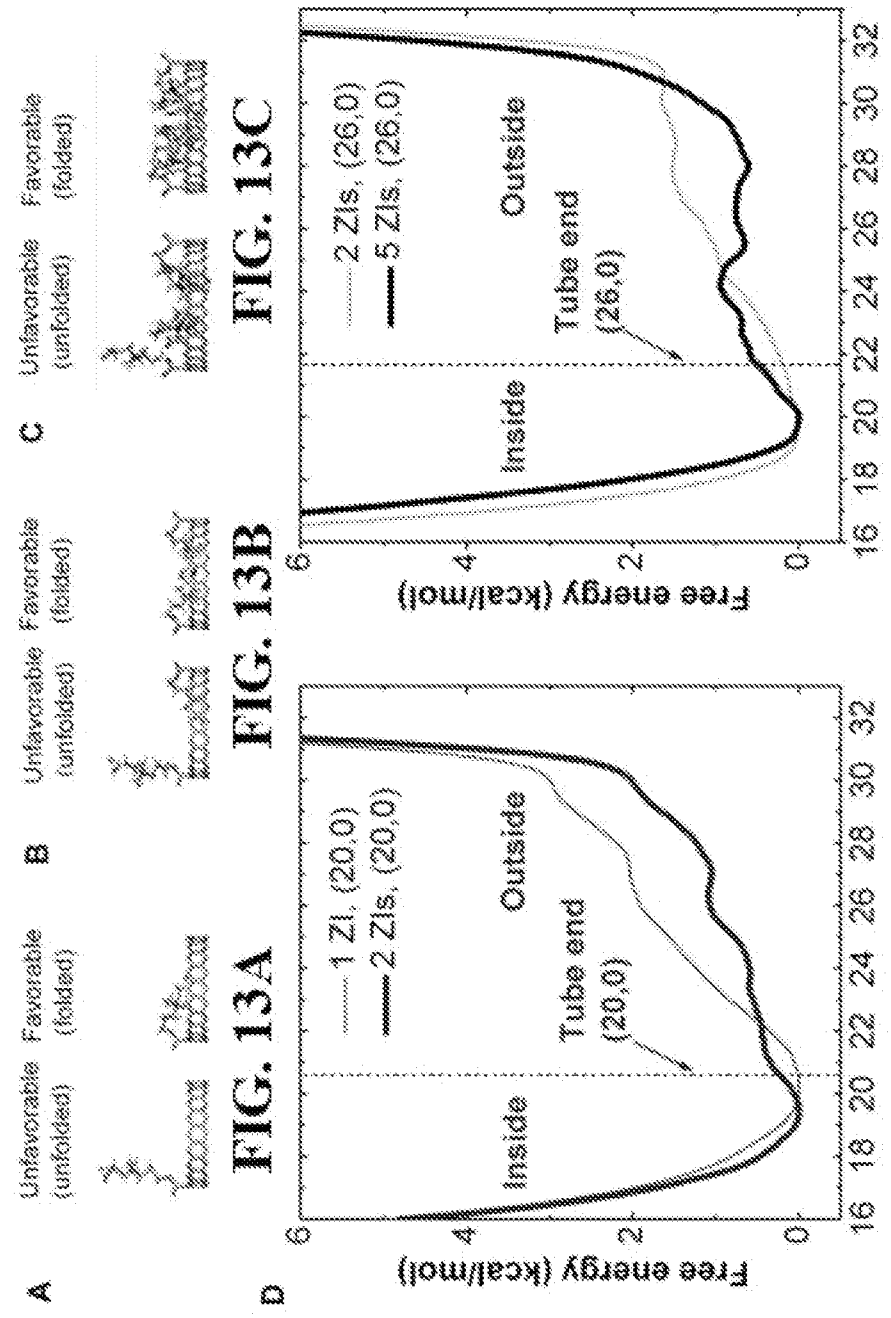

FIG. 13A

FIG. 13B

FIG. 13C

FIG. 13D

FIG. 13E

FIGS. 13A-E

Concentration	Cation conductance	Anion conductance	Total ion conductance	Water conductance	Ion rejection ratio
0.6 M NaCl	3.8 ± 0.2	3.6 ± 0.1	7.4 ± 0.2	460.0 ± 10.7	24.7 % ± 4.3 %
0.3 M NaCl	2.1 ± 0.2	1.9 ± 0.2	3.9 ± 0.4	500.3 ± 20.3	27.4 % ± 9.2 %
0.6 M KCl	2.7 ± 0.2	3.0 ± 0.4	5.7 ± 0.6	489.9 ± 6.3	45.3 % ± 6.3 %
0.3 M KCl	1.3 ± 0.1	1.7 ± 0.2	3.0 ± 0.2	520.4 ± 10.1	45.9 ± 5.4 %

FIG. 14

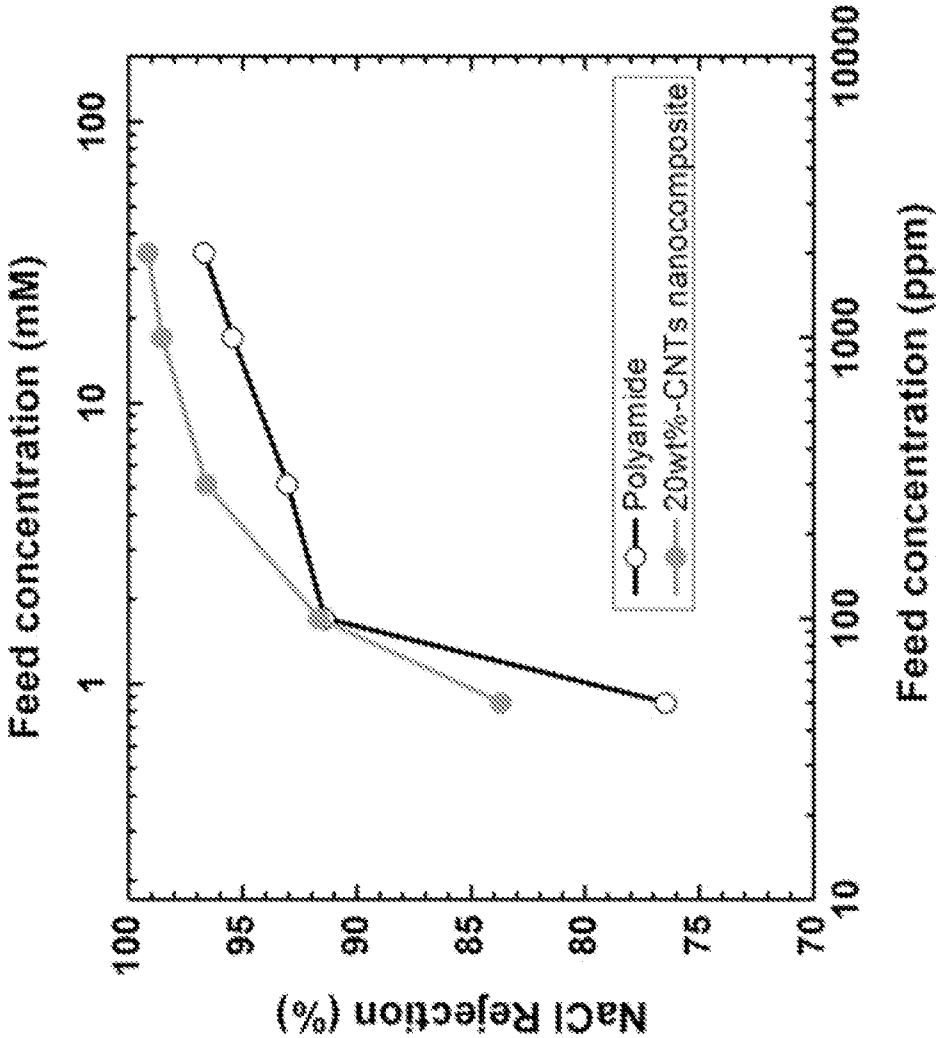
NaCl Rejection (%)
100
95
90
85
80
75
70
Feed concentration (mM)
100
10
1
Feed concentration (ppm)
10000
1000
100
10
Polyamide
20wt%-CNTs nanocomposite

FIG. 15

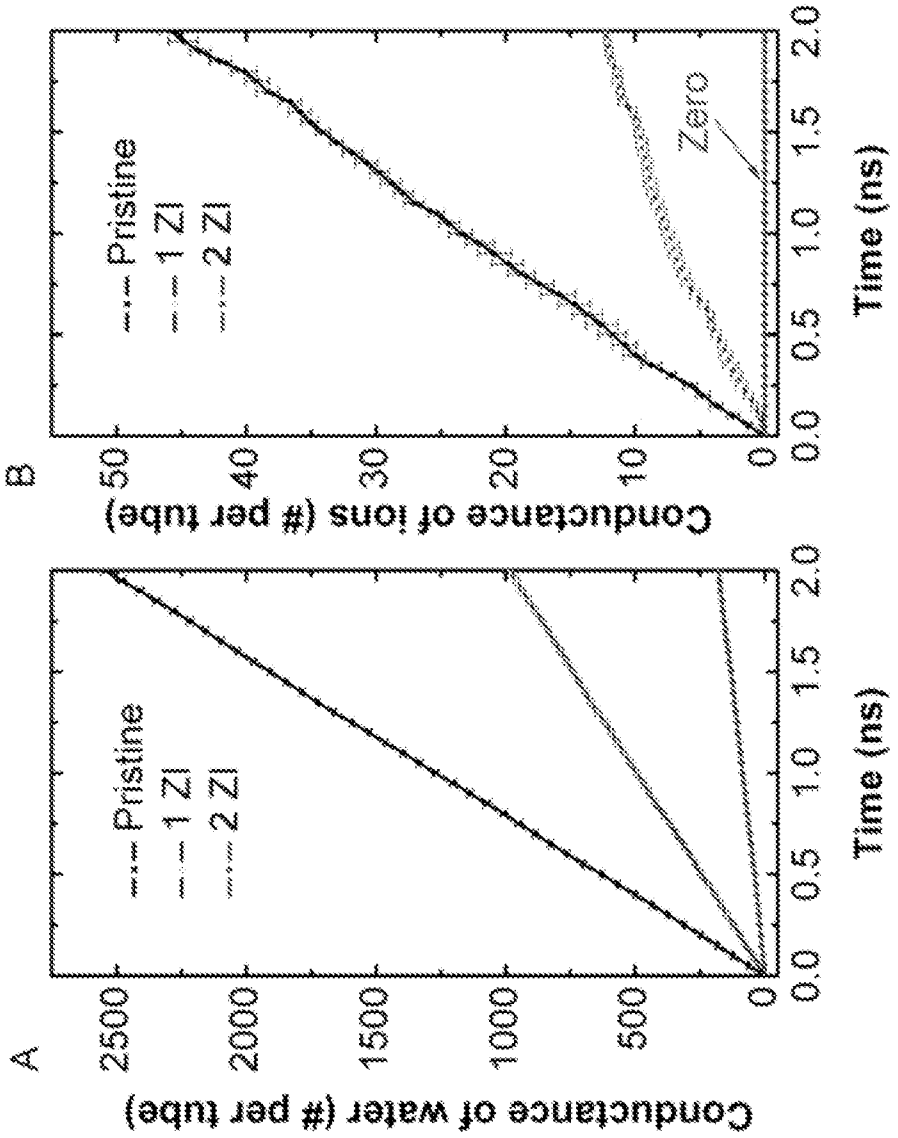

FIG. 16A

FIG. 16B

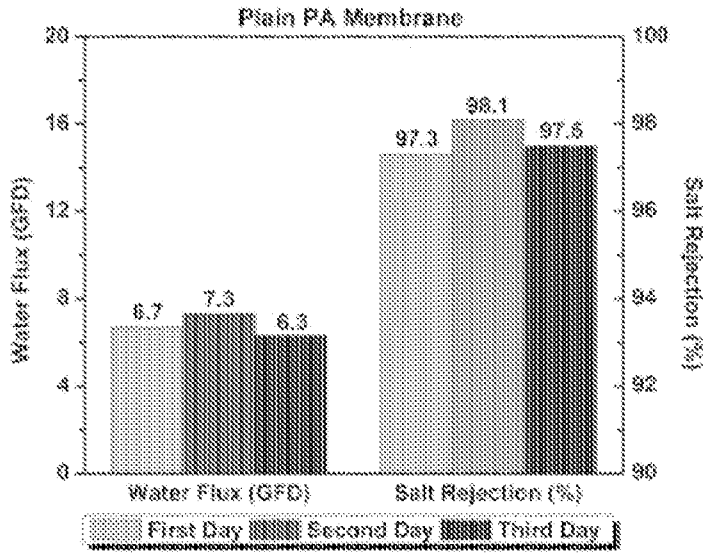

FIG. 17A

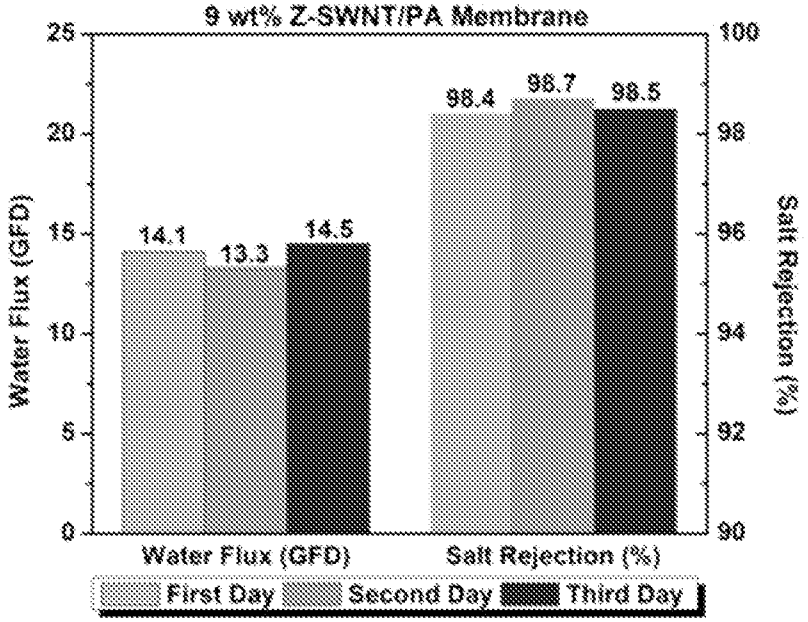

FIG. 17B

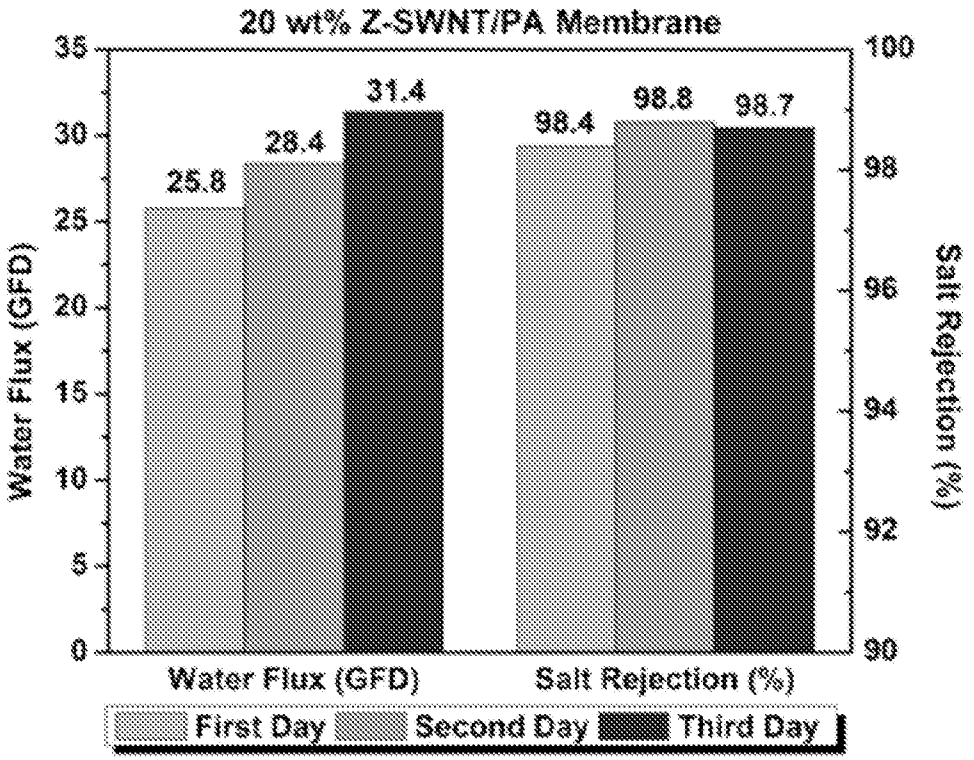
20 wt% Z-SWNT/PA Membrane
Water Flux (GFD)
Salt Rejection (%)
35
30
25
20
15
10
5
0
100
98
96
94
92
90
25.8
28.4
31.4
98.4
98.8
98.7
Water Flux (GFD)
Salt Rejection (%)
First Day
Second Day
Third Day

FIG. 17C

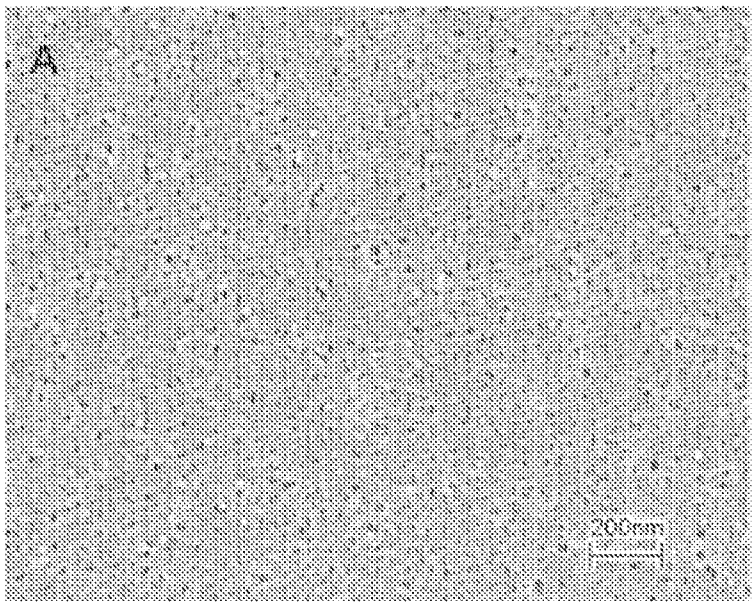

FIG. 18A

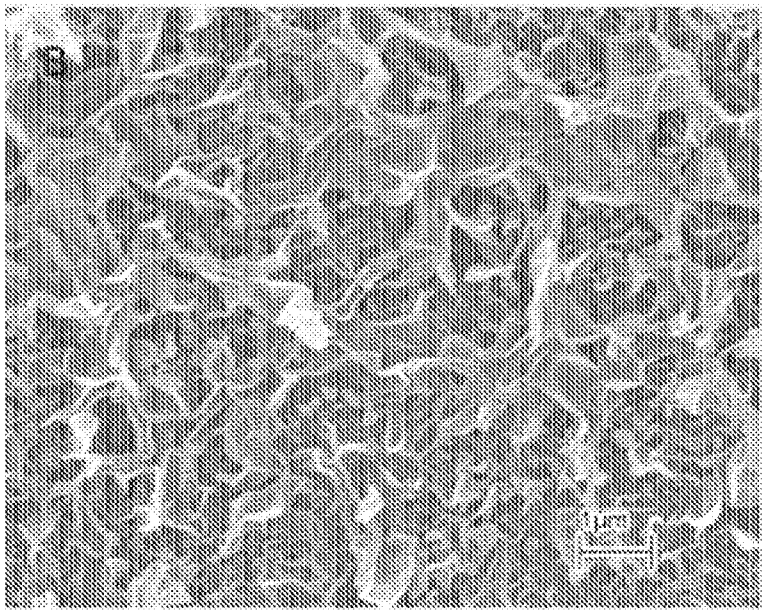

FIG. 18B

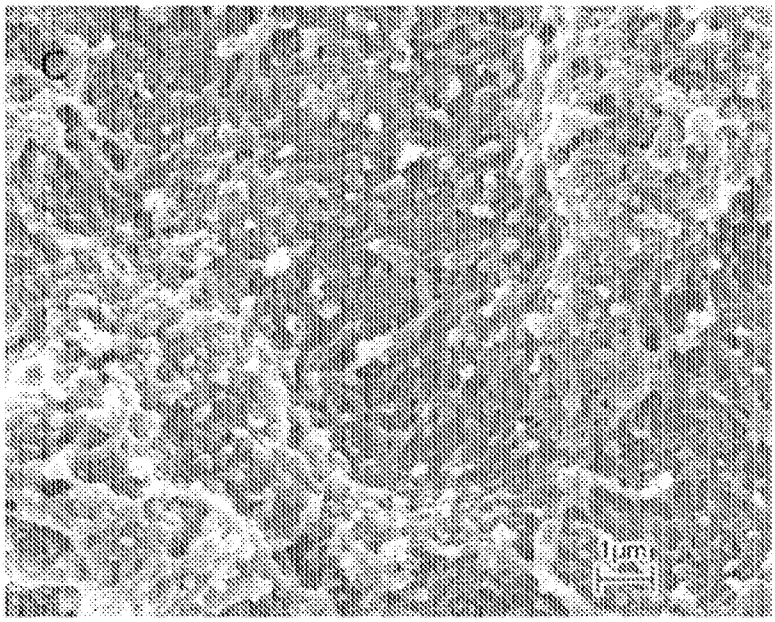

FIG. 18C

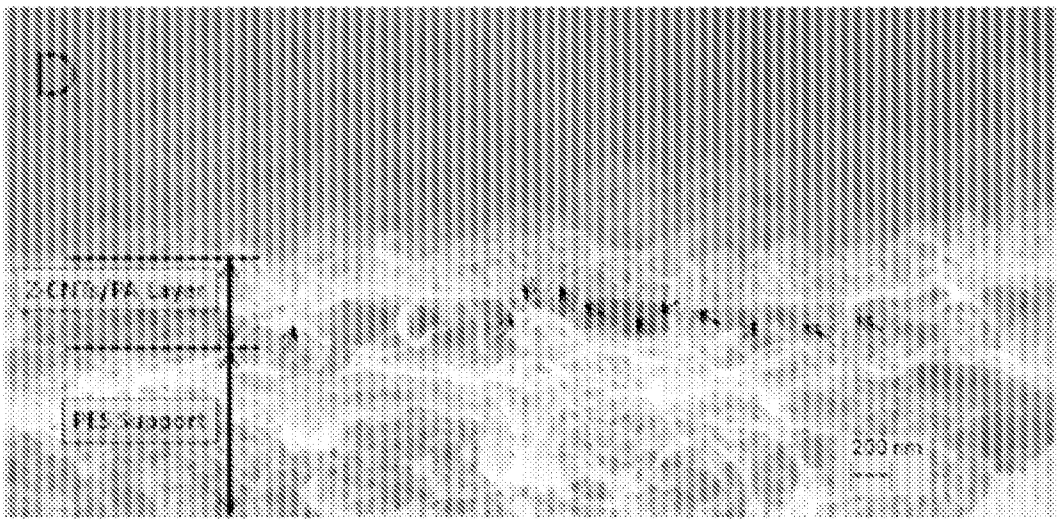

FIG. 18D

INTERNATIONAL SEARCH REPORT

International application No.
PCT/US2013/040744

A. CLASSIFICATION OF SUBJECT MATTER

B01D 69/12(2006.01)i, B01D 71/02(2006.01)i, B01D 69/10(2006.01)i

According to International Patent Classification (IPC) or to both national classification and IPC

B. FIELDS SEARCHED

Minimum documentation searched (classification system followed by classification symbols)

B01D 69/12; B29C 43/02; B01D 39/00; B01D 71/56; H01M 4/86; B01D 71/02; B01D 69/10

Documentation searched other than minimum documentation to the extent that such documents are included in the fields searched
Korean utility models and applications for utility models
Japanese utility models and applications for utility models

Electronic data base consulted during the international search (name of data base and, where practicable, search terms used)

eKOMPASS(KIPO internal) & keywords: functionalized carbon nanotube, fabricating, nanocomposite membrane, zwitterionic, depositing, polymer

C. DOCUMENTS CONSIDERED TO BE RELEVANT

Category*	Citation of document, with indication, where appropriate, of the relevant passages	Relevant to claim No.
X	WO 2007-061945 A2 (NANOSYS INC.) 31 May 2007 See claims 15, 23-24 and 88.	41-43
A		1-40,44-77
A	US 2008-0290020 A1 (MARAND, EVA et al.) 27 November 2008 See claims 1, 2-7, 10, 18 and 20.	1-77
A	US 2005-0040090 A1 (WANG, YONG et al.) 24 February 2005 See claims 1 and	1-77
A	US 2010-0283174 A1 (MA, CHEN-CHI MARTIN et al.) 11 November 2010 See claim 2.	1-77
A	WO 2010-135033 A1 (GENERAL ELECTRIC COMPANY) 25 November 2010) 25 November 2010 See claim 20.	1-77

☐ Further documents are listed in the continuation of Box C.

☒ See patent family annex.

* Special categories of cited documents:
"A" document defining the general state of the art which is not considered to be of particular relevance
"E" earlier application or patent but published on or after the international filing date
"L" document which may throw doubts on priority claim(s) or which is cited to establish the publication date of citation or other special reason (as specified)
"O" document referring to an oral disclosure, use, exhibition or other means
"P" document published prior to the international filing date but later than the priority date claimed
"T" later document published after the international filing date or priority date and not in conflict with the application but cited to understand the principle or theory underlying the invention
"X" document of particular relevance; the claimed invention cannot be considered novel or cannot be considered to involve an inventive step when the document is taken alone
"Y" document of particular relevance; the claimed invention cannot be considered to involve an inventive step when the document is combined with one or more other such documents,such combination being obvious to a person skilled in the art
"&" document member of the same patent family

Date of the actual completion of the international search	Date of mailing of the international search report
13 August 2013 (13.08.2013)	**14 August 2013 (14.08.2013)**

Name and mailing address of the ISA/KR
Korean Intellectual Property Office
189 Cheongsa-ro, Seo-gu, Daejeon Metropolitan City, 302-701, Republic of Korea
Facsimile No. +82-42-472-7140

Authorized officer
LEE Dong Wook
Telephone No. +82-42-481-8163

INTERNATIONAL SEARCH REPORT

Information on patent family members

International application No.
PCT/US2013/040744

Patent document cited in search report	Publication date	Patent family member(s)	Publication date
WO 2007-061945 A2	31/05/2007	AT 528811 T	15/10/2011
		AU 2005-314211 A1	15/06/2006
		AU 2005-314211 B2	08/07/2010
		AU 2006-318658 A1	31/05/2007
		AU 2006-318658 B2	28/07/2011
		CA 2588548 A1	15/06/2006
		CA 2624776 A1	31/05/2007
		CN 101107737 A0	16/01/2008
		CN 101107737 B	21/03/2012
		CN 101563801 A	21/10/2009
		CN 101563801 B	27/03/2013
		CN 101707256 A	12/05/2010
		CN 102593466 A	18/07/2012
		EP 1829141 A2	05/09/2007
		EP 1829141 B1	29/05/2013
		EP 1952467 A2	06/08/2008
		EP 1952467 A4	02/06/2010
		EP 1952467 B1	12/10/2011
		EP 1952467 B9	14/03/2012
		EP 2378597 A1	19/10/2011
		JP 2008-523565 A	03/07/2008
		JP 2009-524567 A	02/07/2009
		JP 2009-524567 T	02/07/2009
		KR 10-2007-0086981 A	27/08/2007
		KR 10-2008-0070769 A	30/07/2008
		KR 20080070769 A	30/07/2008
		US 2006-0188774 A1	24/08/2006
		US 2007-0212538 A1	13/09/2007
		US 2008-0280169 A1	13/11/2008
		US 2009-0017363 A1	15/01/2009
		US 2010-0233585 A1	16/09/2010
		US 7179561 B2	20/02/2007
		US 7842432 B2	30/11/2010
		US 7939218 B2	10/05/2011
		US 7977007 B2	12/07/2011
		US 7977013 B2	12/07/2011
		WO 2006-062947 A2	15/06/2006
		WO 2006-062947 A3	21/12/2006
		WO 2007-061945 A3	30/04/2009
		WO 2007-061945 A9	12/07/2007
US 2008-0290020 A1	27/11/2008	US 7931838 B2	26/04/2011
		WO 2008-028155 A2	06/03/2008
		WO 2008-028155 A3	31/12/2008
		WO 2008-028155 A9	24/04/2008
US 2005-0040090 A1	24/02/2005	AU 2002-367020 A1	30/07/2003
		AU 2002-367020 B2	20/11/2008
		CA 2470025 A1	24/07/2003

INTERNATIONAL SEARCH REPORT

Information on patent family members

International application No.
PCT/US2013/040744

Patent document cited in search report	Publication date	Patent family member(s)	Publication date
		CA 2470025 C	21/02/2012
		EP 1465836 A2	13/10/2004
		EP 2295376 A2	16/03/2011
		EP 2295376 A3	31/10/2012
		US 2003-0116503 A1	26/06/2003
		US 2003-0119920 A1	26/06/2003
		US 2004-0147620 A1	29/07/2004
		US 2006-0167120 A1	27/07/2006
		US 6713519 B2	30/03/2004
		US 6824689 B2	30/11/2004
		US 7008969 B2	07/03/2006
		US 7011760 B2	14/03/2006
		US 7288576 B2	30/10/2007
		WO 03-059813 A2	24/07/2003
		WO 03-059813 A3	23/10/2003
US 2010-0283174 A1	11/11/2010	TW 201041218 A	16/11/2010
WO 2010-135033 A1	25/11/2010	CN 102438735 A	02/05/2012
		JP 2012-527348A	08/11/2012
		KR 10-2012-0028931 A	23/03/2012
		SG 176128A1	29/12/2011
		TW 201105409 A	16/02/2011
		US 2010-0297429 A1	25/11/2010